HHS Public Access

Author manuscript

Cell Host Microbe. Author manuscript; available in PMC 2024 December 13.

Published in final edited form as:

Cell Host Microbe. 2023 December 13; 31(12): 2093–2106.e7. doi:10.1016/j.chom.2023.10.019.

Duffy Antigen is Expressed During Erythropoiesis in Duffy Negative Individuals

Celia Dechavanne[1,10], **Sebastien Dechavanne**[1,10], **Jürgen Bosch**[1,2,10], **Sylvain Metral**[3], **Karli R. Redinger**[1], **Quentin D. Watson**[1], **Arsene, C. Ratsimbasoa**[4,5], **Brooke Roeper**[1], **Sushma Krishnan**[1], **Rich Fong**[1], **Seth Bennett**[1], **Lenore Carias**[1], **Edwin Chen**[6], **Nichole D. Salinas**[7], **Anil Ghosh**[1], **Niraj H. Tolia**[7], **Philip G. Woost**[8], **James W. Jacobberger**[8], **Yves Colin**[3], **Benoit Gamain**[3,*], **Christopher L. King**[1,9,*], **Peter A. Zimmerman**[1,11,*]

[1.]Center for Global Health & Disease, Case Western Reserve University, Cleveland, OH, USA.

[2.]InterRayBio, LLC, Cleveland, OH, USA

[3.]Université Paris Cité and Université des Antilles, INSERM, BIGR, F-75015 Paris, France.

[4.]University of Fianarantsoa, Fianarantsoa, Madagascar.

[5.]CNARP (Centre National d'Application de Recherche Pharmaceutique), Antananarivo, Madagascar.

[6.]Division of Infectious Diseases, Department of Medicine, University of Pittsburgh School of Medicine, Pittsburgh, PA, USA.

[*]**Corresponding authors:** Peter A. Zimmerman, PhD, paz@case.edu, Professor of Pathology, Genetics and Biology, The Center for Global Health & Diseases, Case Western Reserve University, Biomedical Research Building, Room 426, Cleveland, OH 44106-4983, 2109 Adelbert Road, T: 216-368-0508, Christopher L. King, MD, PhD, cxk21@case.edu, Professor of Pathology and Medicine, The Center for Global Health & Diseases, Case Western Reserve University, Biomedical Research Building, Room 429, Cleveland, OH 44106-4983, 2109 Adelbert Road, T: 216-368-4817, Benoît Gamain, PhD, benoit.gamain@inserm.fr, UMR-S 1134, Inserm/Université Paris Cité, 8 rue Maria Helena Vieira Da Silva, 75014 Paris, France, T: +33 1 81 72 43 43.

Author contributions: CD, SD, SM, BG, CLK and PAZ conceived the study; CD and SD wrote the first draft of the paper with PAZ; CD, SD, SM, CLK, BG, PAZ and JWJ developed the flow cytometry design for the bone marrow analysis. JB, QDW and PAZ developed the *P. vivax in vitro* culture methodologies as well as the in vitro invasion experiments. JB, QDW, KR performed all Imagestream analyses and interpretation with PAZ. KR and JB performed all SPR analyses and interpretation. CD, SD; KR and JB performed the competition experiments with red cells. PAZ and ACR developed the Madagascar field studies and protocol development with the Madagascar Ethical Committee. SB conducted all genotyping assays. CD, SD SK, RF, BR and PGW conducted erythrocyte binding assays and flow cytometry. CD, SD and LC conducted western blot analyses. AG produced unfolded rPvDBPII. NHT, EC and NDS synthesized rPvDBPII. YC developed and provided 2C3 and CA111. SM, SD and BG conducted *in vitro* proliferation, expansion, and differentiation of CD34+ cells. BG, CLK and PAZ oversaw all aspects of the study. CD, SD, JB, BG, CLK and PAZ analyzed the results.

Ethics approval and consent to participate

Study protocols were approved by the University Hospitals of Cleveland Institutional Review Board (#08-03-33 and #09-90-195) and the Madagascar Ethical Committee (No. 099-MSANP/CE).

Consent for publication

All authors read and approved the final manuscript.

Competing interests

The authors have declared that no conflict of interest exists.

Declaration of Interests

The authors declare no competing interests.

[7]Host-Pathogen Interactions and Structural Vaccinology Section, Laboratory of Malaria Immunology and Vaccinology, National Institute of Allergy and Infectious Diseases, National Institutes of Health, Bethesda, MD, USA

[8]Case Comprehensive Cancer Center Flow Cytometry Core, Case Western Reserve University.

[9]Veterans Affairs Research Service, Cleveland, OH, USA

[10]These authors contributed equally

[11]Lead contact

Summary

The erythrocyte silent Duffy blood group phenotype in Africans is thought to confer resistance to *Plasmodium vivax* blood-stage infection. However, recent studies report *P. vivax* infections across Africa in Fy-negative individuals. This suggests that the GATA-1 SNP underlying Fy-negativity does not entirely abolish Fy expression or that *P. vivax* has developed a Fy-independent red blood cell (RBC) invasion pathway. We show that RBCs and erythroid progenitors from *in vitro* differentiated CD34 cells and from bone marrow aspirates from Fy-negative samples express a functional Fy on their surface. This suggests that the GATA-1 SNP does not entirely abolish Fy expression. Given these results, we developed an *in vitro* culture system for *P. vivax* and show *P. vivax* can invade erythrocytes from Duffy-negative individuals. This study provides evidence that Fy is expressed in Fy-negative individuals and explains their susceptibility to *P.* vivax with major implications and challenges for *P. vivax* malaria eradication.

Graphical Abstract

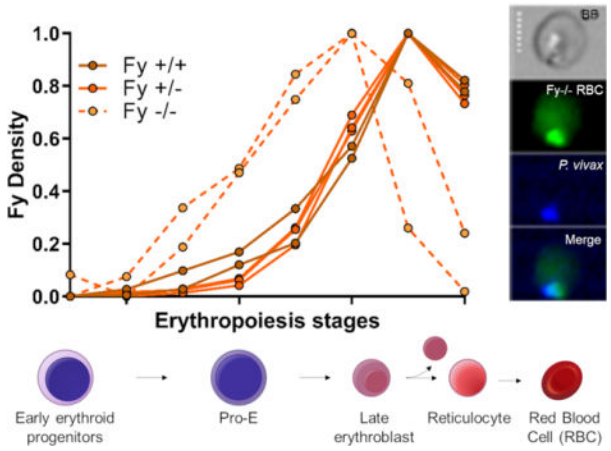

eTOC blurb

The Duffy gene (*Fy*) polymorphism has historically been linked to *Plasmodium vivax* natural susceptibility/resistance, but clinical infections have recently been detected in *Fy*-negative individuals. Dechavanne and colleagues observe Fy expression during early erythropoietic stages in *Fy*-negative individuals, which enables *P. vivax* invasion and helps explain infections seen in *Fy*-negative individuals.

Keywords

Duffy protein; Duffy negative individuals; Erythroid Progenitors; *Plasmodium vivax* ; Bone marrow

Introduction

Duffy gene (*FY*) polymorphism has been prominent historically. In 1968, Donahue *et al.* used Fya/Fyb serological inheritance patterns and human chromosome 1 centromeric staining features to make *FY* the first gene mapped to a human autosome[1]. Functionally, the Duffy blood group protein (Fy)[2] also known as Duffy antigen chemokine receptor (DARC) or CD234, was the first identified member of the diverse seven-transmembrane chemokine receptor family, albeit with several interesting structural and functional differences that make its biology unique[2]. Fy expression on both erythroid and non-erythroid cells[2] modulates homeostatic levels and gradients of chemokines between blood circulation[3–7] and tissues[8–12].

The decades-long observations that Africans and African Americans, who are for the most part Fy-negative, were highly resistant to *Plasmodium vivax* blood-stage infection[13–18] suggested that interaction with the Fy protein was required for parasite invasion of human red blood cells (RBCs)[19]. *P. vivax*, selectively invades reticulocytes in a process that requires region II of *Plasmodium vivax* Duffy-binding protein (rPvDBPII) with DARC receptor[20–26]. With gene sequencing, a single nucleotide polymorphism (SNP) in the *FY* gene GATA-1 transcription factor binding site has been shown to inhibit *FY* erythroid expression[27,28] and homozygosity underlies the “Fy erythrocyte silent” (herein, Fy-negative) phenotype characterized by standard serological methods[27]. *In vitro* studies using Fy-dependent *P. knowlesi*[20,29] show that while the merozoite can orient apically to the RBC surface, the parasite failed to invade Fy-negative erythrocytes. Therefore, the onward formation of a tight mobile junction needed for infection of the RBC failed[30]. This background has inextricably linked Duffy blood group genetics and malaria. Recent studies now report *P. vivax* infections in Fy-negative individuals from many malarious African countries[31,32]. These observations lead to at least two hypotheses. First, constitutive low-level or periodic Fy expression may occur in Fy-negative people and facilitate occasional blood-stage infection. Second, *P. vivax* may not interact with Fy exclusively and has developed a Fy-independent RBC invasion pathway. Even if other *P. vivax* proteins appear to play a role in parasite invasion[33,34] (e.g., reticulocyte-binding proteins) no alternative pathway has been so far identified.

Previous studies have demonstrated a gene dosage effect of the *FY* GATA-1 SNP that reduces erythrocyte surface expression of Fy^a and Fy^b by 50% in heterozygous individuals[28,35], and others have identified additional coding region SNPs associated with reduced expression of both Fy^a (Fy^a-weak)[36] and Fy^b (Fy^b-weak)[37–39]; very rare nonsense SNPs and deletions in the *FY* gene coding region have also been reported (see text with Supplemental Information (SI) Table S1)[40,41]. Further, Fy is more highly expressed on reticulocytes versus older RBCs[35]. With this range of Fy expression phenotypes, we tested the hypothesis that the GATA-1 SNP (FY^{ES} mutation) may not entirely block Fy protein

expression and here we describe how this may influence susceptibility to *P. vivax* blood stage infection.

Results

Fy expression on Fy-positive and Fy-negative pbRBC

To assess the presence of Fy on peripheral blood red blood cells (pbRBC), two anti-Fy6 antibodies were used: the conventional mouse monoclonal antibody 2C3[42,43] and the camelid single-domain antibody CA111[44], which overlaps the binding site of 2C3 and possess a higher affinity[45]. We tested whether the anti-Fy6 antibodies recognized Fy on the surface of Fy-negative ($FY*B^{ES}/*B^{ES}$) and Fy-positive RBC (Figures S1, S2 and S3). Working on freshly collected pbRBC, we observed CA111 binding to pbRBC of *FY*A/*A*, *FY*B/*B* donors and $FY*B^{ES}/*B^{ES}$ pbRBC at different time points (Figure 1A). Collection of different time points from the same donors indicated variations in CA111 binding from 74.0% to 89.4% for *FY*B/*B* pbRBC, 77.2% to 90.8% for *FY*A/*A* pbRBC and 11.5% to 47.6% for $FY*B^{ES}/*B^{ES}$. This latter result was markedly higher than previously observed on $FY*B^{ES}/*B^{ES}$ donors[44]. Another set of experiments was performed using the conventional anti-Fy6 2C3 and the single-domain anti-Fy6 CA111 (Figure 1B) and anti-Fya and anti-Fyb on 10 other Fy-negative donors (Figure 1C). CA111 detected Fy on the pbRBC from *FY*B/*B* (N=7) and $FY*B^{ES}/*B^{ES}$ donors (N=10, Figure 1B) confirming the observation of Figure 1A. Using the 2C3, Fy protein was detected on the pbRBC of *FY*B/*B* donors but not on the $FY*B^{ES}/*B^{ES}$ donors. As expected, the anti-Fya antibody showed reactivity on pbRBC from *FY*A/*B* donor only and the anti-Fyb antibody on *FY*A/*B and FY*B/*B* pbRBC. Taken together, these results suggest that the Fy protein is consistently detected on the pbRBC surface of $FY*B^{ES}/*B^{ES}$ by CA111 compared to 2C3 and the anti-Fya and anti-Fyb antibodies used for clinical serology and detection of Fy is in a reduced range in Fy-negative compared to Fy-positive individuals.

rPvDBPII binding on $FY*B^{ES}/*B^{ES}$ pbRBC

Given the unexpected interaction of the CA111 Fy6-specific antibody with $FY*B^{ES}/*B^{ES}$ pbRBC, we tested in additional experiments the host-parasite functionality of the Fy protein by evaluating rPvDBPII binding to pbRBC. As expected, a high binding of rPvDBPII on *FY*A/*B* pbRBC was observed, while a much lower binding of rPvDBPII was also observed on $FY*B^{ES}/*B^{ES}$ pbRBC (Figure 2A). We then exposed both Fy-positive and Fy-negative pbRBC to rPvDBPII, washed and eluted pbRBC bound proteins and then probed them with a polyclonal antibody to PvDBP as previously described[46,47]. This specific detection revealed a single protein band of approximately 35kDa - consistent with the detection of the rPvDBPII protein – from both $FY*B^{ES}/*B^{ES}$ and *FY*A/*B* pbRBC on a Western blot (Figure 2B).

Given historically consistent demonstration of the chymotrypsin-sensitive nature of the Fy protein[20,48–51], we then tested the reproducibility of rPvDBPII binding to both *FY*A/*B* and $FY*B^{ES}/*B^{ES}$ pbRBC after chymotrypsin treatment. We examined the chymotrypsin sensitivity of rPvDBPII binding for one *FY*A/*B* and one $FY*B^{ES}/*B^{ES}$ (Donor #1) at multiple independent times. Results consistently showed that the binding of rPvDBPII

to both *FY*A/*B* and *FY*B^{ES}/*B^{ES}* pbRBC were significantly higher before than after chymotrypsin treatment (Figure 2C).

To further evaluate the relative affinity of rPvDBPII interaction to Fy-positive and Fy-negative pbRBC, we tested the dissociation of PvDBPII from pbRBC with increasing NaCl concentrations (Figure 2D). While we observed that the relative binding of rPvDBPII to *FY*B^{ES}/*B^{ES}* pbRBC was markedly lower than that observed for *FY*B/*B* and *FY*A/*B*, dissociation of rPvDBPII from *FY*B/*B* and *FY*A/*B* versus *FY*B^{ES}/*B^{ES}* pbRBC had a similar pattern across increasing NaCl concentrations (0.15M, 0.3M, 0.6M and 1M NaCl). At 1.5M NaCl the pbRBC for all *FY* genotypes were lysing and therefore rPvDBPII signal decreased across all samples.

In a more specific test of rPvDBPII binding to Fy-positive and Fy-negative pbRBC, we compared the binding of properly folded rPvDBPII to partially denature rPvDBPII (same amino acid construct) on pbRBC (Figure 2E). Results showed that irrespective of the Duffy genotype, denatured rPvDBPII (dark boxes) compared to properly folded (light boxes) had significantly reduced binding to Fy-positive and Fy-negative pbRBC. Taken together these results show that rPvDBPII bind specifically to Fy-positive and Fy-negative pbRBC and are consistent with CA111 anti-Fy6 binding experiments.

Variable rPvDBPII binding on pbRBC over time

To observe the persistence of the interactions between rPvDBPII and pbRBC over time, we examined multiple samples from both Fy-positive and Fy-negative study participants in a time-course study (Figure 3A). The pbRBC samples were collected and examined over 282 days for one *FY*B/*B* donor (orange), one *FY*A/*A* donor (green) and two *FY*B^{ES}/*B^{ES}* donors (red and blue). Among the *FY*B^{ES}/*B^{ES}* pbRBC sampling time points (7 samples for both *FY*B^{ES}/*B^{ES}* #1 (red) and *FY*B^{ES}/*B^{ES}* #2 (blue)), five samples showed rPvDBPII binding at least 2-fold above the negative control; both *FY*B^{ES}/*B^{ES}* donors showed evidence of rPvDBPII binding 5-fold above the negative control. The variability observed in rPvDBPII binding among the Fy-negative donor samples was also observed for both Fy-positive donors (regardless of their genotype). Overall, the rPvDBPII binding (mean fold-increase over negative control and range) was 32.4 for *FY*B/*B* (1.8 –110.9), 17.2 for *FY*A/*A* (4.9–47.7), 1.9 for *FY*B^{ES}/*B^{ES}* #1 (0.7 – 5.9), 2.4 for *FY*B^{ES}/*B^{ES}* #2 (0.5 – 6.7). Interestingly, across this series of samples from the four pbRBC donors featured, the higher levels of Fy expression on *FY*B^{ES}/*B^{ES}* pbRBC were comparable to the lower level of rPvDBPII binding for the *FY*A/*A* pbRBC (Figure 3A). As further evidence of Fy protein expression on the *FY*B^{ES}/*B^{ES}* pbRBC surface, we were able to immunoprecipitate, after solubilizing the pbRBC membranes, the Fy protein using CA111 anti-Fy6 and detected it using the commercial anti-Fy [ACKR1] antibody (Figure 3B).

To further confirm the specificity of rPvDBPII binding to pbRBC in this time-course study, we used both CA111 and nDARCIg (a chimeric protein including Fy and IgG1-Fc region[52]) in competition assays to block rPvDBPII access to the RBC. The Fy-specific CA111 nanobody (Figure 3C **left panels**) decreased rPvDBPII binding from 25.2-fold (range, 5.8;110.9) over negative controls to 2.1-fold (0.2;12.1) for both Fy-positive donors (P-value =0.001 for *FY*B/*B*; P-value =0.001 for *FY*A/*A*). Under the same conditions, rPvDBPII

binding decreased from 2.0-fold (0.5;6.4) over negative controls to 0.8-fold (0.2;1.9) for both Fy-negative donors (P-value =0.002 for *FY*B*^{ES}/*B^{ES} #1; P-value =0.003 for *FY*B*^{ES}/*B^{ES} #2). In the partner experiments (Figure 3C **right panels**), nDARCIg was observed to decrease rPvDBPII binding to Fy-positive pbRBC from 25.2-fold (5.8; 110.9) over negative controls to 2.81-fold (0.5;7.7) (P-value=0.005 for *FY*B/*B*; P-value=0.005 for *FY*A/*A*). For the *FY*B*^{ES}/*B^{ES} pbRBC, nDARC decreased rPvDBPII binding to pbRBC from 2.0-fold (0.5;6.4) over negative controls to 1.0-fold (0.3;2.8) (statistically significant P-values all <0.05 for both *FY*B*^{ES}/*B^{ES} samples). Thus, both CA111 and nDARCIg blocked the binding of rPvDBPII to *FY*B*^{ES}/*B^{ES} pbRBCs, providing evidence of Fy-specific binding of rPvDBPII to *FY*B*^{ES}/*B^{ES} pbRBC.

Fy protein expression on erythroid progenitor cells *in vitro*

Given a wide range of results pointing to *P. vivax* preference for infection of reticulocytes[53–61] and the apparent low, variable expression of Fy protein on *Fy*B*^{ES}/*B^{ES} pbRBC (Figures 1A, 1B and 3A), we postulated that this expression pattern reflects the declining Fy expression on older pbRBC[35]. Indeed, recent evidence from murine studies showing that the Fy protein is expressed at higher levels on pro-erythroblasts and normoblasts, compared to mature RBC[62]. We initiated these *in vitro* studies by expanding CD34^{pos} (expressed on megakaryocyte erythrocyte progenitors[63–67]) from the peripheral blood of one *FY*B/*B* donor and *FY*B*^{ES}/*B^{ES} Donors #1 and #2[63]. At Days 11, 15 and 18 of differentiation, cells were collected to monitor erythroid lineage maturation using the surface markers CD36, CD71, Glycophorin A and Band 3 and query Fy protein expression (Figure 4A and Figure 4B). As expected, during the differentiation process, CD36 and CD71 were decreasing, whereas Glycophorin A and Band 3 increased among the most mature RBCs. No difference in the maturation stages from the different donors was observed over time (Figure 4A). Expression of the Fy protein during these differentiation time points was monitored by either flow cytometry (CA111 binding, Figure 4B) and/or Western blot (CA111 immunoprecipitation; anti-ACKR1 detection, Figure 4C and FigureS4). For the *FY*B/*B* donor, at Day11, 48.9% of the cell population expressed the Fy protein at the cell surface whereas from Day15 to Day18 >96% of the population expressed the Fy protein. From the two different *FY*B*^{ES}/*B^{ES} donors, the expression of the Fy protein was observed *in vitro* as early as Day11 of maturation. Consistent with our previous results on pbRBC, the Fy protein expression was lower on *FY*B*^{ES}/*B^{ES} cells (11.1 and 35.5%) than on *FY*B/*B* cells (48.9%). However, we observed that significantly higher proportions of the erythroid precursor cells from *FY*B*^{ES}/*B^{ES} donors tested positive for the Fy protein by Day18 (49.7% for *FY*B*^{ES}/*B^{ES} #1 and 83.8% for *FY*B*^{ES}/*B^{ES} #2) (Figure 4B) than was observed previously for pbRBC (highest proportion of Fy-positive pbRBC from Figure 3A - 6% for *FY*B*^{ES}/*B^{ES} #1 and 7% for *FY*B*^{ES}/*B^{ES} #2). Expression of the Fy protein on erythroid precursors differentiated *in vitro* at Day18 was further confirmed by immunoprecipitation and Western blot (Figure 4C).

The same *in vitro* differentiation was performed on human bone marrow aspirates (HBMAs)[63]. From expanded CD34^{pos} bone marrow cell populations of both Fy-positive and Fy-negative samples, we were also able to immunoprecipitate and detect the Fy protein (Figure 4D).

These studies confirm the ability of individuals with *FY*B*^{ES}*/*B*^{ES} genotype to express the Fy protein in erythroid progenitor cells cultured *in vitro*. Nevertheless, these results required confirmation of Fy expression in erythroid progenitor cells *ex vivo*.

Ex vivo Fy protein expression on bone marrow erythroid precursors.

Fy expression was evaluated *ex vivo* with CA111 anti-Fy6 (n=5 Fy-positive, n=2 Fy-negative) and rPvDBPII (n=2 Fy-positive, n=2 Fy-negative) binding on erythroid precursor cells from bone marrow samples (Figure 5). On the same samples, we monitored the expression of the following cell surface markers as accepted indicators of erythroid precursors: CD34[63–67], CD45 (marker to differentiate erythroid from lymphoid development[64]), CD105 (marker of human erythrocyte progenitor (hEP)[67–69]), and CD71 (transferrin receptor preferentially expressed on young reticulocytes[70]) (Figure 5A). The cell size and expression of these markers on bone marrow subpopulations were similarly observed among all Fy phenotypes. We further assessed Fy protein expression in bone marrow erythroid precursors using CA111 and rPvDBPII recognition (Figure 5B). The highest levels of anti-Fy6 binding was observed within the CD34^{neg}/CD45^{neg}/CD105^{mid}/CD71^{pos} subpopulation (skewed toward reticulocytes; CD105 declining) for Fy-negative donors and CD34^{neg}/CD45^{neg}/CD105^{neg}/CD71^{pos} subpopulation for Fy-positive donors. Further detailed comparative analyses of bone marrow samples from individuals representing specific *FY* genotypes are provided in Figures S5 and S6.

Finally, we confirmed expression of Fy protein by CA111-capture and commercial anti-ACKR1-detection from both Fy-negative and Fy-positive donors in the erythroid precursor bone marrow population (Figure 5C; Figure S7).

P. vivax in vitro invasion into Fy-positive and Fy-negative erythroid cells.

With the Fy protein detected by Fy-specific antibodies and rPvDBPII on genotypically Fy-negative erythroid cells, we determined whether cryopreserved *P. vivax* field isolates (asynchronous) would interact with and/or invade host cells. Short-term invasion assays used peripheral blood of North American Fy-positive and Fy-negative participants as target cells seeded with stock *P. vivax* cells. In order to distinguish between *P. vivax* re-infection of stock culture cells and new invasion into target cells, we labeled the target cell populations with CFSE (carboxyfluorescein succinimidyl ester). Imagestream analyses were performed after 72 hours of culture. Overall assessment of the RBC invasion experiments by imaging flow cytometry provides an overview for selecting populations of cells down to assessments of individual parasite-target cell interactions (Figure 6, Figure S8, S9, S10 and S11, Table S2). Figure 6A shows separation of single cells (black data points) versus multiple (gray data points) cells by aspect ratio and area in the brightfield image. Results in Figure 6B show that strategic CSFE labeling of target RBCs in a control cell population without exposure to parasites serving as a background control. Results from the invasion assays show newly infected Fy-positive and Fy-negative target cells (CFSE+ and Hoechst+) in Figures 6C and 6D, respectively. To confirm *P. vivax* infected target cells, we examined individual cells of interest (circled cells) with bright field and fluorescent images (Figure 6C and 6D), with Fy-positive target cells (Figures 6E1–6 correspond to circled/numbered cells in Figure 6C) and Fy-negative target cells (Figures 6F1–6 correspond to circled/numbered

cells in Figure 6D). These results show *P. vivax* merozoites interacting with and invading Fy-positive (Figures 6E1 to 6E4) and Fy-negative (Figures 6F1 to 6F4) target cells. Figures 6E5 & 6F5 are uninfected donor cells (stock culture) and Figures 6E6 & 6F6 are infected donor cells (stock culture). Our experiments also show that cells from *FY*B/*B* compared to $FY*B^{ES}/*B^{ES}$ donors are more readily invaded by *P. vivax* by a factor of 2.2 (Table S2).

Discussion

Given our findings on *P. vivax* infection of Fy-negative people from Madagascar[71,72] and reports from other malarious sites across Africa[31,32,73], we wanted to investigate how parasite and host invasion proteins interacted with Fy-negative RBCs. We therefore assessed whether or not two different anti-Fy6 antibodies and rPvDBPII bind to the surface of different erythroid target cells (pbRBC; expanded CD34 cell populations; bone marrow). Our data show that Fy is expressed at the surface of pbRBC and this expression is variable in both Fy-negative and Fy-positive individuals. Using competitive inhibition studies, we demonstrated that adding of CA111 or nDARCIg significantly reduced rPvDBPII binding to Fy-positive pbRBC and essentially blocked rPvDBPII binding to Fy-negative pbRBC. These results suggest that rPvDBPII binding is focused on the anti-Fy6 epitope and thus limited to the Fy protein.

Our initial studies on pbRBC, showed that Fy expression on Fy-negative pbRBC was positive at some sample collection time points and that these pbRBC could interact with rPvDBPII at levels similar to RBC from *FY*A/*A* people. Because of *P. vivax* preference for infection of reticulocytes[33,53–60], we studied Fy expression across a broader time frame of erythroid development. Human and murine studies show higher levels of Fy protein expression on pro-erythroblasts, normoblasts and reticulocytes compared to mature RBC[35,58,62]. Additionally, Malleret *et al.* have demonstrated that immature reticulocytes ($CD71^{pos}$), mostly found in the bone marrow and matured in the spleen[59] are preferentially invaded by *P. vivax* compared to older reticulocytes and erythrocytes ($CD71^{neg}$), than in the peripheral blood. Recent studies emphasize that the bone marrow and especially the spleen, the latest accounting for more than 98% of the estimated total-body *P. vivax* biomass, are important reservoirs of *P. vivax* infection in humans and non-human primate model systems[74–76]. Since the spleen harbor more mature reticulocytes than in the bone marrow, the distribution of the *P. vivax* biomass is inconsistent with the relative paucity of invasion-receptive reticulocytes in the spleen. One possibility could be that upon *P. vivax* infection, the erythropoiesis within the bone marrow is impaired, resulting in extramedullary hematopoiesis (EMH)[77] induction within the spleen and then allowing the expansion of parasite biomass beyond the bone marrow. With this focus on the importance of reticulocytes as *P. vivax* invasion-targets, interactions between reticulocyte binding proteins and CD71 and CD98 heavy chain suggest additional molecular components of the *P. vivax* erythrocyte invasion mechanism[78].

Our studies on earlier erythroid stages focused on enriching $CD34^{pos}$ megakaryocyte erythrocyte progenitors that circulate in the peripheral blood, allowing them to mature *in vitro* under conditions favoring erythroid development[63]. We purposefully performed a time-course study on the same Fy-negative donors to evaluate the variability of erythroid

precursors released in the peripheral circulation over time. Interestingly, results showed that significantly higher proportions of the erythroid precursor cells from *FY*B*^{ES}*/*B*^{ES} donors were positive for Fy protein detection than their pbRBC.

With the observation of Fy protein expression from the CD34 cell maturation experiments, we repeated our studies on bone marrow aspirate samples as the site for natural erythroid cell development and also an important reservoir of *P. vivax*. We monitored the expression of CD34, CD45, CD105 and CD71 expression as markers distinguishing erythroid from lymphoid maturation. Results from these bone marrow studies showed Fy protein expression on early-stage cells committing to erythroid development in both Fy-positive and Fy-negative people. Our observations suggest that Fy expression initiates in an early erythroid subpopulation (CD34^{pos}/CD45^{pos}/CD105^{mid}/CD71^{neg}) in both Fy-positive and Fy-negative people. Because Fy expression drops for Fy-negative individuals whereas the expression increased for Fy-positive individuals, we speculate that, before proerythroblast differentiation and transition to GATA-1[68,79], Fy expression may be driven by another transcription factor, such as GATA-2 and this may contribute to the results we have observed. Consistent with Tournamille *et al.* findings (i.e., compromised *FY* gene expression associated with the GATA-1 *FY*^{ES} SNP)[27], the amount of Fy protein begins to decay earlier in Fy-negative than in Fy-positive erythroid cells. The observed decline of Fy signal in CD34^{neg}/CD45^{neg}/CD105^{mid}/CD71^{pos} cells, appears to be consistent with RBC extrusion of its nucleus, after which RBC precursors are no longer able to express their genes and the cell can only be equipped with the gene products expressed prior this important developmental event.

The potential that bone marrow could be the source of reticulocytes for *in vitro* cell culture is becoming an increasingly important area of *P. vivax* research. Fernandez-Becerra *et al.* have expanded CD34^{pos} hematopoietic stem cells to generate CD71^{pos} reticulocytes for *in vitro P. vivax* culture[80]. We followed in this direction by using human bone marrow aspirates from US donors, to provide target cells for *in vitro* propagation of *P. vivax* field isolates from the Madagascar communities where we have previously observed significant frequency of Fy-negative *P. vivax* infections[71,72]. Human bone marrow aspirates have enabled *in vitro* propagation of two field isolates as source parasite material for the short-term invasion assays presented here. Using these *in vitro* propagated *P. vivax*, we have shown that both Fy-positive and Fy-negative RBCs can be invaded by *P. vivax*.

Limitations

Although our work provides a clear demonstration that the dogma about Fy-negative individuals no longer holds and represents significant advances for understanding *P. vivax* malaria, we recognize limitations that future studies should address. While we have shown that *P. vivax* can invade Fy-negative cells *in vitro*, it was not possible to demonstrate that RBC invasion was Fy protein dependent and completely rule out the possibility that *P. vivax* can use an alternative invasion pathway. With the development of monoclonal antibodies and peptide-based inhibitors, interrupting interactions between PvDBP, PvEBP2, PvRBP and other *P. vivax* merozoite proteins, more specific invasion inhibition studies are warranted. For this to occur, it will be necessary to refine *P. vivax in vitro* invasion studies to allow

more extensive studies. The demonstration of *P. vivax* invasion of Fy-negative cells *in vitro* opens potential that laboratory-adapted *P. vivax* strains could be used to study a range of candidate protein-protein interactions necessary for blood stage infection. Additionally, while the focus of our experiments provided assessment of Fy expression from multiple different sample types (pbRBC; expanded CD34 cell populations; bone marrow aspirates), we were not able to examine Fy-expression from splenic reticulocytes of Fy-negative and Fy-positive individuals. Emerging studies that have probed *P. vivax* infections outside of the peripheral blood are critically important to advance current perspectives on *vivax* malaria pathogenesis and evaluate Fy genotype variation in future studies of this nature.

Conclusions

Our results provide a mechanism to explain why Fy-negative people are not completely resistant to *P. vivax* blood-stage malaria[3,4] by showing that Duffy antigen can be variably expressed in subjects with the GATA1 polymorphism associated with Fy negativity. With the peak of Fy expression during early reticulocyte stages and declining as RBCs enter peripheral circulation, our findings support observations that the bone marrow and sites of extramedullary erythropoiesis are important for *P. vivax* blood stage propagation. Our results are consistent with observations that *P. vivax* infections in Fy-negative individuals are usually detected by PCR, not blood smear microscopy. *P. vivax* infection in Duffy negative individuals expands human populations potentially capable of *P. vivax* transmission. Our results also raise questions regarding *P. vivax* malaria pathogenesis, especially given a wide range of clinical observations showing bone marrow involvement, from *in vitro* studies[78,81], individual case histories[82–84] and cohort studies[85–87]. With potential significant involvement of the bone marrow, it becomes easier to understand how considerable anemia and other markers of hematological disruption are out of proportion with low levels of observed *P. vivax* peripheral blood parasitemia (summarized in Baird[33] and Silva-Filho et al.[88]). Given evidence that peripheral blood infections significantly underestimate the total body biomass of a *P. vivax* infection and therefore global prevalence, closer examination of *P. vivax* infection and disease biomarkers (lactate dehydrogenase and other circulating parasite antigens)[88,89] is required to more accurately estimate the burden of vivax malaria in Fy-negative Africa and globally.

STAR Methods

RESOURCE AVAILABILITY

Lead contact—Further information and requests for resources and reagents should be directed to and will be fulfilled by the lead contact, Peter A. Zimmerman (paz@case.edu).

Materials availability—Proteins generated in this study will be shared by the lead contact upon request if necessary with a Material Transfer Agreement.

Data availability—Any additional information required to reanalyze the data reported in this paper will be available from the lead contact upon request.

EXPERIMENTAL MODEL AND SUBJECT DETAILS

Study Participants and Sample Collection—Study protocols were approved by the University Hospitals of Cleveland Institutional Review Board (#08-03-33 and #09-90-195). All methods were carried out in accordance with guidelines and regulations included within our protocols. Informed consent was obtained from all subjects, and for subjects who were under 18, from a parent and/or legal guardian. Eleven Fy-positive (three females and eight males) and sixteen Fy-negative persons (nine females and seven males) were included (Table S1); all Fy-negative persons were homozygous for the negative GATA-1 mutation (rs2814778; $FY*B^{ES}/*B^{ES}$). All blood and bone marrow samples were processed within 2 hours of collection.

METHOD DETAILS

DNA Extraction and PCR-based Genotyping—All study participants were genotyped by previously described methods[71]. Genomic DNA was extracted from the whole blood samples using the QIAGEN QIAmp DNA Blood Kit following recommended protocols with a starting blood volume of 200 μL and an elution volume of 200 μL of Buffer AE (Valencia, CA).

PCR amplifications of Duffy blood group gene sequences were performed in reaction mixtures (28μL) with 3 μL of genomic DNA, 180 μM each dNTP, 67mM Tris-HCl (pH 8.8), 6.7 mMMgSO4, 16.6mM$(NH_4)_2$SO4, 10mM 2-mercaptoethanol, 0.1 μM each primer (Primers inclusive of promoter (rs2814778) and *FY*A*/*FY*B* (rs12075) snps - forward primer, Duffy-200up 5′-CAGGCAGTGGGCGTGGG-3′; reverse primer, Duffy +730dn 5′-CTGCTAGCTAGGATACCCAG-3′; Primers inclusive of *FY*B*/*FY*X* (rs34599082) snp - forward primer, FYBXup 5′-AGCACTGTCCTCTTCATGCTTT-3′; reverse primer, FYBXdn 5′-GCAGAGCTGCGAGTGCTAC-3′) and 2.5 units of thermostable DNA polymerase under the following conditions: 95 °C for 2min, followed by 40 cycles of 95 °C (30 s), 60 °C (30 s), and 72°C (90 s) and a final extension at 72 °C (5 min) (PCR products 912 and 1,033 bp). Following PCR amplification, products were further processed by a ligation detection reaction (LDR). The LDR was performed in a reaction mixture (15 μL) containing 20mMTris-HCl buffer (pH 7.6), 25 mM potassium acetate, 10mM magnesium acetate, 1mM NAD+, 10mM DTT, 0.1% Triton X- 100, 13nM each LDR probe,1 μL of PCR product, and 2 units of Taq DNA ligase (New England BioLabs). LDR probes consisted of six allele-specific oligonucleotides and three fluorescently labeled conserved-sequence oligonucleotides. The allele-specific probes contained an MTAG sequence for further hybridization with complementary sequence oligonucleotides bound to Luminex FlexMAP fluorescent microspheres; conserved-sequence probes were 5′ phosphorylated and 3′ biotinylated.

Sequences of the LDR probes used were as follows: Duffy null promoter snp (rs2814778) at nucleotide −67 (t, wild-type; c, erythrocyte silent): PRO ntT MTAG_A018: 5′-ACACTTATCTTTCAATTCAATTACcattagtccttggctcttat-3′ PRO ntC MTAG_A020: 5′-CTTTCTCATACTTTCAACTAATTTtcattagtccttggctcttac-3′ PRO common: 5′-phosphate-cttggaagcacaggcgctg-biotin-3′.

Codon 42 snp (rs12075) associated with Fya and Fyb phenotypes (g, Fya; a, Fyb): *FY*A* ntG MTAG-A022: 5′-CAAACAAACATTCAAATATCAATCttcccagatggagactatgg-3′ *FY*B* ntA MTAG-A026: 5′- TACATTCAACACTCTTAAATCAAActtcccagatggagactatga-3′ Codon42 common: 5′-phosphate-tgccaacctggaagca-biotin-3′.

Codon 89 snp (rs34599082) associated with Fyb or the Fyb^{weak} phenotypes (c, Fyb; t, Fyb^{weak}): *FY*B* ntC MTAG-A028: 5′-CACTTAATTCATTCTAAATCTATCtgcttttcagacctctctcc-3′ *FY*X* ntT MTAG-A034: 5′- ACTTATTTCTTCACTACTATATCAtgcttttcagacctctctct-3′ Codon89 common: 5′-phosphate-gctggcagctctgccctggct-biotin-3′.

Protein expression

CA111 anti-Fy nanobody: Variable domain of a heavy chain only (VHH), nanobody of camelids. This nanobody includes the CA52 VHH sequence[44] and an HA (human influenza virus hemagglutinin)-tag. This nanobody was kindly provided by Olivier Bertrand (National Institute of Blood Transfusion (INTS), Paris, France)[44]. CA111 was obtained by subcloning the CA52 VHH sequence into a Novagen pET 28-b derived plasmid allowing expression in the cytoplasm of SHuffle (C3029H) cells. This plasmid encodes (from 5' to 3') a polyhistidine tail, a thrombin cleavage site, the VHH, and an HA-tag; it is used for routine subcloning of other VHHs using the PstI and Eco91I sites[90].

The resulting nanobody exhibits the following characteristics.

- Interferes with the interleukin-8 binding to Fy on RBCs.
- Interferes with P. vivax infection of red blood cells (short term culture).
- Upon linkage to a solid substrate, this nanobody acts as a powerful adsorbent to purify native Fy in a single step from a detergent extract of cells.
- Pepscan analysis identified 22**FEDVW**26 as the peptide sequence of the linear epitope.

A single dromedary was immunized with the N-terminal extracellular domain constructs of Fy expressed in E. coli (referred to as ECD1; Amino acids 6 [H] to 63 [P] – HRAELSPSTENSS **QLDFED**VWNSSYGVNDSFPDGDY[G/D]ANLEAAAPCHSCNLLDDSALP)[44]. This domain covers the region to which Fy6 epitope, chemokines and the P. vivax Duffy binding protein (PvDBP) bind (amino acids 19 to 25 – 19**QLDFEDV**25) and carries the polymorphic G/D site at amino acid 42, responsible for the Fya/Fyb allotypes. From the immunized animal, a VHH library of dromedary lymphocytes was exposed to ECD1 to yield several Fy-specific VHHs. Smolarek et al. focused on one VHH, referred to as CA52. The linear epitope of CA52 exhibits capacity to recognize the glycosylated Fy protein present on human cells, although the immunogen was a non-glycosylated polypeptide.

To further validate the specificity of the CA111 antibody, we assessed its reactivity on K562 cells expressing or not the Fy antigen and Saimiri RBC[91]. Blood samples (2 mL) from

Bolivian squirrel monkeys (S. boliviensis), collected in EDTA vacutainers, was obtained from the Biologics Production Program, Michael E. Keeling Center for Comparative Medicine and Research, The University of Texas MD Anderson Cancer Center (Protocol number: 00000451-RN01-AR001). The blood was shipped on ice overnight and used in our studies on the day of arrival.

rPvDBPII recombinant protein—Region II of Salvador I strain PvDBP (rPvDBPII; 37.6 KDa) was expressed as inclusion bodies in Escherichia coli and then refolded and purified as previously described[21–23]. The protein purified before refolding served as a negative control.

Duffy Antigen Receptor for Chemokine chimeric protein construct (nDARCIg Fyb)—Briefly, as previously described[52], HEK293H cells were co-transfected with pCDM8-DARC-Fc (first N-terminal 60 amino acids of Fy) and pRc/CMV-TPST (human sulfotransferase).

Fy detection by flow cytometry—Erythrocyte binding assays were performed based on previously developed strategies and reagents[46,47]. Peripheral blood RBC (1×10^6) from human or Saimiri) or K562 cells[92] were first blocked for 30 min with PBS 1% BSA. Anti-Fy antibodies were then incubated for 20 min at 37°C at the following concentrations: CA111 (30 μg/mL), murine monoclonal antibody, 2C3 (10 μg/mL)[42,43], anti-FyA (ref: 808 186 BioRad, 1:10 dilution) or anti-FyB (ref: 808 191 BioRad, 1:10 dilution) antibodies. A mouse anti-HA antibody (Biolegend; 30 μL of a 1:1000 dilution in PBS 0.2% BSA; 20 min at 37°C) followed by a goat-anti-mouse PE-conjugated antibody (eBioscience; 40 μl of a 1:80 dilution in PBS 0.2% BSA; 20 min at 37°C in the dark) for CA111, an anti-mouse for 2C3 or an anti-human for anti-Fy antibodies were used to detect the binding. Following 2 washes in PBS 0.2% BSA, a total of 100,000 cells (all samples in triplicate) were analyzed by flow cytometry. Between each staining step, pbRBC were washed two times with PBS 0.2% BSA. For *ex vivo* fresh bone marrow samples, a direct anti-HA tag phycoerythrin (PE)- tagged antibody was used to reduce the background (Miltenyi, dilution 1:11). Similar procedures were followed for other Fy-specific antibody reagents. For the experiments on the maturation of CD34+ hematopoietic stem cells, the same protocol was performed and at least 50,000 cells were analyzed by flow cytometry. In evaluation of bone marrow precursors, the BSA concentration change from 1% to 2% and at least 500,000 cells were evaluated to ensure sufficient data capture for erythroid precursor subpopulations of interest.

rPvDBPII binding monitored by flow cytometry—Peripheral blood RBC (1×10^6) were first blocked for 30 min with PBS 1% BSA and then further incubated with rPvDBPII Sal1 (20μg/mL final concentration; 60 μL of a 1:20 dilution in PBS 0.2% BSA; 30 min at 37°C). After 2X washes with PBS 0.2%BSA, these cells were incubated with a rabbit polyclonal anti-PvDBP serum (30 μL of a 1:50 dilution in PBS 0.2% BSA; 20 min at 37°C). Cells were washed again 2X with PBS 0.2%BSA and then incubated with rabbit phycoerythrin (PE)-tagged antibody (Sigma; 40 μL of a 1:32 dilution in PBS 0.2% BSA; before 20 min at 37°C in the dark). After 2 washes in PBS 0.2% BSA and a final wash in PBS, cells were subjected to analytical flow cytometry[46,47]. Erythrocyte binding assays were further optimized by adjusting the blocking concentrations for BSA.

Unfolded rPvDBPII was used as the same concentration as folded rPvDBPII and the protocol is identical.

Erythrocytes were pre-treated with chymotrypsin (1 mg/mL) 30 min at 37 °C. The enzyme treatment was stopped by washing five times with PBS 0.2% BSA. A blocking step (1% BSA for an hour at 37°C) were performed before rPvDBPII binding.

For the rPvDBPII dissociation assessment, the rPvDBPII binding protocol as described above was performed and increasing NaCl concentrations from 0.15M to 1.0M were added 750 µL of each gradually. The measures were acquired on Attune NTX.

Competition assays

Blocking of rPvDBPII binding: the competition assay was performed using pre-incubated erythrocytes with CA111 (30 µg/mL) or nDARCIg (60 µg/mL) for an hour at 37°C before rPvDBII binding following the same steps as described above.

Blocking of CA111 binding: the competition between CA111 and 2C3 was performed on fresh FY **B/*B* pbRBC, FY $*B^{ES}/*B^{ES}$ pbRBC or enriched reticulocytes from FY $*B^{ES}/*B^{ES}$ donor. The enrichment protocol was described elsewhere[93]. Briefly, after leucocyte depletion using NWF syringe filter, cells were resuspended in 3 ml high-KCl buffer (pH 7.4) and then incubated 20 minutes at room temperature on a rocker. After centrifugation, cells were resuspended in 500 µL of high-KCl buffer and layered over 300 ul 19% Nycodenz-KCl solution in a 1.1 mL microtube. Tube was centrifuged at 3,000g for 30 min without braking. Reticulocytes at the interface were harvested and washed 2 times in PBS. After a blocking step, cells were pre-incubated with increasing concentrations of CA111 (molar ratio from 0 to 25) an hour at 37°C. 2C3 was then directly added (no wash) at 5 µg/mL. The detection of the 2C3 binding was following the same steps as described above.

rPvDBPII Erythrocyte Capture Assay—This assay was previously described[85]. Briefly, ~10^6 cells were collected from packed RBC and 10 µg of recombinant PvDBPII was added. After 2 hours of incubation at room temperature, the preparation was layered on top of 500 µL of dibutylphtalate and centrifuged at 11,000 rpm for 30 sec. The pellet was collected, and the proteins bound at the RBC surface were eluted adding 20 µL of 1.5 M NaCl drop wise and shaking. After incubation (5 min), this procedure was repeated with 1.0 M of NaCl and then 0.3 M of NaCl. The preparation was centrifuged at 14,000 rpm for 2 min. The proteins present in the supernatant were separated on a Tris-Glycine SDS 4–20% gel (Biorad) in reducing conditions and then transferred onto a PVDF membrane. The membrane was blocked for one hour with TBS 0.1% tween, 5% milk, incubated with rabbit anti-PvDBPII (1: 2,000), washed, then followed by the secondary antibody anti-rabbit HRP (Thermo Scientific). Chemiluminescent signal was detected using SuperSignal (Pierce) on X-ray film.

Fy immunoprecipitation by CA111 and Western Blot detection

Solubilization and protein extraction –: Packed RBC (~5 mL); cells matured during the *in vitro* erythroid differentiation; and CD45 negative sorted-cells from the bone marrow were

lysed by three cycles of freeze/thaw followed by sonication. After adding 5 mM Tris·HCl, pH 8.0 with protease inhibitor (Sigma Aldrich), the protein preparation was centrifuged 20 min at 16,000 × g at 4°C. The pellet was resuspended twice in 0.1 M Na_2CO_3 pH 11.5 with protease inhibitor and centrifuged 20 min at 16,000 × g at 4°C. To solubilize the membrane proteins from the pellet, 1mM triton X100 + protease inhibitors were added and incubated at room temperature for 30 min.

Immunoprecipitation of Fy antigen -: CA111 was covalently coupled to magnetic beads (Dynabeads M-270 Carboxylic Acid, Invitrogen) for 30 min at room temperature with slow rotation. EDC at 100mg/ml (1-ethyl-3-[3-dimethylaminopropyl] carbodiimide) was dissolved 100mM MES (2-(N-morpholino) ethanesulfonic acid)) buffer (pH 5.0) for the activation reaction and incubated for 2 hr at 4°C with slow rotation. The solubilized extract was incubated with the activated beads for 1h. Beads were resuspended in Laemmli buffer for SDS gel and western blot.

Western blot -: The beads + extract solutions were separated on a Tris-Glycine SDS 4–20% gel (Biorad) in reducing conditions and were then transferred onto a PVDF membrane. The membrane was blocked for one hour with TBS 0.1% Tween 5% milk. Polyclonal rabbit anti-ACKR1 (2ug/ml; LS Bioscience) and HRP anti-rabbit antibody (diluted 1/10,000 into 10 ml TBS 0.1% Tween 5% milk; Thermo Scientific) were used to probe Fy from the immunoprecipitated elution. The signal was detected on X-ray films using SuperSignal (Pierce).

Specificity of CA111 -: Tests of specificity were performed on recombinant proteins by direct Western blotting, or immunoprecipitating cells from patient bone marrow and subsequent Western Blot. For the direct probe of the Western Blot, 0.1 μg of nDARCIg and rCXCR2 were loaded on a gel; 0.2 μg/mL of CA111 were used to probe the Western blot and reveal the signal. For the immunoprecipitation experiment, 0.5 μg of rCXCR2 were used. The anti-CXCR2 antibody (R&D system, 0.5 μg/mL) was used to probe recCXCR2 on a Western Blot as a positive control.

Erythroid differentiation of CD34 positive cells—Isolation of CD34 positive cells was performed from peripheral blood donors (*FY*B/*B* and $FY*B^{ES}/*B^{ES}$ donors; #1 and #2) and from bone marrow samples. Mononuclear cells were isolated by Ficoll Plaque Plus (GE Healthcare) and frozen in 10% DMSO. The thawed cells were positively selected for CD34 by magnetic beads (human CD34 MicroBead Kit; Miltenyi Biotech). Between 10,000 and 100,000 cells were obtained after selection and differentiated in culture over 21 days. A detailed protocol is published by Jingping Hu *et al.*[63]. The *in vitro* differentiation was monitored by flow cytometry with 400,000 cells per day (Day 11, Day 15, Day 18) monitoring surface markers CD36 (BD Biosciences), CD71 (BD Biosciences), Band 3 (American Research Product) and Glycophorin A (Life Technology).

Monitoring maturation and expansion of CD34+ Hematopoietic Stem Cells (HSCs).—Mononuclear cells were isolated by Ficoll Paque Plus (GE Healthcare) and frozen in 10%DMSO. The thawed cells were positively selected for CD34 by magnetic beads (human CD34 MicroBead Kit; Miltenyi Biotech). Between 10,000 and 100,000 cells

were obtained after selection and differentiated in culture over 21 days. A detailed protocol is published by Jingping Hu *et al*[63]. For the *FY*B/*B* donor and 2 $FY*B^{ES}/*B^{ES}$ donors, the cells were counted by light microscopy during the *in vitro* differentiation at different time points (Day 0, 11, 15 and 18).

The *in vitro* differentiation was monitored by flow cytometry with 400,000 cells per day (Day 11, Day 15, Day 18) monitoring the presence/absence of the surface markers CD36 (BD Biosciences), CD71 (BD Biosciences), Band 3 (American Research Product) and Glycophorin A (Life Technology). As expected, during the differentiation process, the cells are losing the CD36 and CD71 expressions whereas Glycophorin A and Band 3 are increasing. Overall, the cells from all the donors were observed to be at comparable stages over time.

Bone marrow cell preparation and staining—Fresh bone marrow was collected in heparin. Erythroid precursors from fresh bone marrow samples were isolated by Ficoll Paque Plus (GE Healthcare) separation. Cells were first blocked for 30 min with FcR blocking reagent (Miltenyi – 20 μL per sample) following manufacturer's recommendations. rPvDBPII and CA111 binding experiments were performed as described above. Sub-populations of erythroid precursors were defined using directly-labeled antibodies - anti-CD45 PerCP Cy5.5 (Becton Dickinson), anti- CD34 FITC, anti-CD105 APC, anti-CD71 APC Cy7 (all from Biolegend) and an anti-Band3 PE (American Research Product). Data were acquired with a BD Biosciences LSR II (San Jose, CA) or a Thermo Fisher Attune Nxt (Waltham, MA) operated within manufacturer's specifications, which was tested with performance beads. To ensure sufficient relevant data, we aimed to acquire 500,000 cell events. Data were analyzed with FlowJo 10.0 (Becton Dickison & Company (BD), Ashland, OR) or WinList 9.0 (Verity Software House, Topsham, ME). Two types of analysis were performed.

Flow cytometric analysis of erythroid progenitor subpopulations in bone marrow—Forward scatter (FSC-A) and side scatter (SSC-A) plots were used to select erythroid populations then standard gating was done to select positive and negative population from orthogonal quadrants on bivariate plots or univariate histograms. For each of the samples analyzed, unstained cells were used to evaluate cell auto-fluorescence. Unstained and single antibody stained cells, or unstained or single stained antibody-binding beads, were used to set fluorescence compensation. Negative controls for CD234 (Fy) were "secondary only" with either CA111 or rPvDBPII omitted in otherwise complete assays. Secondary and tertiary reagents were PE labeled anti HA-tag for CA111and PE labeled goat anti-rabbit, respectively for rPvDBPII (with a polyclonal rabbit anti- PvDBP as secondary antibody). Results collected following comparisons with these negative controls allowed for calculating fold-increase of the geometric mean of fluorescence intensity (CA111 or rPvDBPII) over the negative control or for calculating the fraction of positive cells.

Second, for data collected on bone marrow samples, we analyzed a subset of bone marrow donors to show the level of expression of CD34, CD45, CD105, CD71, and Fy. The antibodies and staining protocol was as above. However, the sub-populations were gated multi-dimensionally using a series of bivariate plots to create a sequential series of erythroid

differentiation states. The fluorescence value of each parameter was divided by a correlated measure of cell size (forward scatter) providing a measure of antigen density. The expression level of Fy was made more accurate by subtracting the fluorescence of the negative control on a subpopulation basis (median fluorescence – median background fluorescence).

Erythroid cell protein extraction and Western blot analysis—Extracting the Fy protein from the surface of erythroid cells was conducted to specifically capture evidence of FY gene expression. These experiments were performed on pbRBCs from Fy-positive and Fy-negative donors. Target cell populations included pbRBC, expanded CD34 cell populations and bone marrow. Details of protein extraction, immunoprecipitation and Western blot analyses are provided earlier in the Star Method.

Competition assay of CA111 or 2C3 binding to Fy-negative RBCs in the presence of nDARC (Fc conjugated DARC)—Blood derived from three Fy negative individuals was incubated with soluble nDARC to compete with the binding to RBC bound DARC. Samples were taken on multiple days and each time tested in quadruplicates for each nDARC concentration (range: 1000 nM to 0.48 nM, twofold serial dilutions) as well as N=12 for 1000 nM nDARC, 0 nM nDARC and 2nd antibody staining alone for higher statistical power. Samples from the three individuals were tested on three different days. Samples were collected on an Attune Next using the appropriate lasers for HO, PE and FITC as well as Forward Scatter and Side Scatter. For each sample, 200,000 events were collected.

Imagestream Analysis—Samples from invasion experiments were collected on an Imagestream IS100 instrument. Target cells were labeled with CFSE, while the donor cells were CFSE negative. Each experiment was seeded using peripheral blood of North-American Fy-positive or Fy-negative participants as target cells and stock *P. vivax* isolates (stock culture: AMP2016.14 and AMP2016.36) at a ratio of 80% to 20% (or 90% to 10%) respectively for a total RBCs 7.2×10^7. After 72h incubation the cells were stained with Höchst 33342 and then fixed with 4 % PFA in 1 × PBS. For each data file 200K events were collected, for most samples we performed four technical replicate (resulting to ~1000K events). All datasets were collected in Extended Depth of Field (EDF) mode, resulting in an extended depth of field when focusing the cells. Only focused cells were further analyzed by first separating them by Area and Aspect Ratio in the brightfield channel, allowing the distinction of single versus multiple cells in an image. Single cells were then separated by intensity in CFSE and HO staining. Five areas are distinguished in the CFSE/HO plot. Unlabeled uninfected donor cells (CFSE-/HO−), infected donor cells (CFSE-/HO+), uninfected labeled target cells (CFSE+/HO−), infected target cells (CFSE+/HO+) and white blood cells (CFSE+/HO>10^5). The HO positive cells detected in the donor cell population versus the uninfected donor cells reflect the parasitemia of that individual sample at the time of collection. In addition, a cutoff value was determined based on a CI95 level of the mean fluorescent intensity of uninfected cells (HO channel). Cells that were above that threshold were deemed positive.

QUANTIFICATION AND STATISTICAL ANALYSIS

Statistical analyses were performed using STATA version 13.0 and are described on the legend of each concerned figure. Additionally, Graphpad Prism 10 was used for statistical analysis of the SPR data as well as the competition assay. Imagestream data was analyzed by the IDEAS Software version 6.2.

Supplementary Material

Refer to Web version on PubMed Central for supplementary material.

Acknowledgments

We are grateful to the study donors who patiently participated over the course of this investigation in the United States and in Madagascar. We are also grateful to the Madagascar study team members, Rosalind E. Howes, Thierry Franchard, Tovonahary Angelo Rakotomanga and Brune Ramiranirina for recruitment of Malagasy study participants, collection, cryopreservation and cataloging of *P. vivax*-infected blood samples. We thank David N. Wald, Director of the Hematopoietic Biorepository & Cellular Therapy Core and Basabi Maitra for recruitment of bone marrow donors. Howard Meyerson, Keith E. Shults and the Comprehensive Cancer Center of Case Western Reserve University and University Hospitals of Cleveland generously contributed to the flow cytometry study design and provided technical support. We thank Chetan Chitnis for providing nDARCIg; Olivier S. Bertrand and Sylvie Cochet (INSERM/University Paris Diderot) for the gift of anti-Fy antibodies (2C3 and CA111) and objective criticisms integral to this study; Anne-Lyse Baudrier, Emmanuel Collec and the Centre National de Reference pour les Groupes Sanguins (CNRGS) for providing the anti-FyA and anti-FyB antibodies.

Funding

This study was funded by grants from the Veterans Affairs Research Service (BX001350) to CLK, NIH Grant (R01 AI064687 and R01 AI143694) to CLK and an NIH Grant (R01 AI097366 and R01 AI148469) to PAZ and the Agence Nationale de la Recherche (ANR-11-LABEX-0024-01 ParaFrap) to BG. N.H.T. and N.D.S are supported by the Intramural Research Program of the National Institute of Allergy and Infectious Diseases, National Institutes of Health.

Availability of data and materials

The datasets used and/or analyzed during the current study are available from the corresponding author on reasonable request.

References

1. Donahue RP, Bias WB, Renwick JH, and McKusick VA (1968). Probable assignment of the Duffy blood group locus to chromosome 1 in man. Proceedings of the National Academy of Sciences 61, 949–955. 10.1073/pnas.61.3.949.
2. Bachelerie F, Ben-Baruch A, Burkhardt AM, Combadiere C, Farber JM, Graham GJ, Horuk R, Sparre-Ulrich AH, Locati M, Luster AD, et al. (2014). International Union of Pharmacology. LXXXIX. Update on the Extended Family of Chemokine Receptors and Introducing a New Nomenclature for Atypical Chemokine Receptors. Pharmacol Rev 66, 1–79. 10.1124/pr.113.007724. [PubMed: 24218476]
3. Darbonne WC, Rice GC, Mohler MA, Apple T, Hébert CA, Valente AJ, and Baker JB (1991). Red blood cells are a sink for interleukin 8, a leukocyte chemotaxin. J Clin Invest 88, 1362–1369. 10.1172/JCI115442. [PubMed: 1918386]
4. Dawson TC, Lentsch AB, Wang Z, Cowhig JE, Rot A, Maeda N, and Peiper SC (2000). Exaggerated response to endotoxin in mice lacking the Duffy antigen/receptor for chemokines (DARC). Blood 96, 1681–1684. [PubMed: 10961863]

5. Neote K, Darbonne W, Ogez J, Horuk R, and Schall TJ (1993). Identification of a promiscuous inflammatory peptide receptor on the surface of red blood cells. J Biol Chem 268, 12247–12249. [PubMed: 8389755]

6. Reutershan J, Harry B, Chang D, Bagby GJ, and Ley K (2009). DARC on RBC limits lung injury by balancing compartmental distribution of CXC chemokines. Eur J Immunol 39, 1597–1607. 10.1002/eji.200839089. [PubMed: 19499525]

7. Vergara C, Tsai YJ, Grant AV, Rafaels N, Gao L, Hand T, Stockton M, Campbell M, Mercado D, Faruque M, et al. (2008). Gene encoding Duffy antigen/receptor for chemokines is associated with asthma and IgE in three populations. Am J Respir Crit Care Med 178, 1017–1022. 10.1164/rccm.200801-182OC. [PubMed: 18827265]

8. Hub E, and Rot A (1998). Binding of RANTES, MCP-1, MCP-3, and MIP-1alpha to cells in human skin. Am J Pathol 152, 749–757. [PubMed: 9502417]

9. Middleton J, Neil S, Wintle J, Clark-Lewis I, Moore H, Lam C, Auer M, Hub E, and Rot A (1997). Transcytosis and surface presentation of IL-8 by venular endothelial cells. Cell 91, 385–395. 10.1016/s0092-8674(00)80422-5. [PubMed: 9363947]

10. Pruenster M, Mudde L, Bombosi P, Dimitrova S, Zsak M, Middleton J, Richmond A, Graham GJ, Segerer S, Nibbs RJB, et al. (2009). The Duffy antigen receptor for chemokines transports chemokines and supports their promigratory activity. Nat Immunol 10, 101–108. 10.1038/ni.1675. [PubMed: 19060902]

11. Rot A (1992). Endothelial cell binding of NAP-1/IL-8: role in neutrophil emigration. Immunol Today 13, 291–294. 10.1016/0167-5699(92)90039-A. [PubMed: 1510812]

12. Zarbock A, Schmolke M, Bockhorn SG, Scharte M, Buschmann K, Ley K, and Singbartl K (2007). The Duffy antigen receptor for chemokines in acute renal failure: A facilitator of renal chemokine presentation. Crit Care Med 35, 2156–2163. 10.1097/01.ccm.0000280570.82885.32. [PubMed: 17855830]

13. O'Leary PA (1927). Treatment of neurosyphilis by malaria: report on the three year's observation of the first one hundred patients treated. Journal of the American Medical Association 89, 95–100. 10.1001/jama.1927.02690020019007.

14. Boyd MF, and Stratman-Thomas WK (1933). Studies on benign tertian malaria. 4. On the refractoriness of negroes to inoculation with Plasmodium vivax. American Journal of Epidemiology 18, 485–489. 10.1093/oxfordjournals.aje.a117964.

15. Young MD, Ellis JM, and Stubbs TH (1946). Studies on imported malarias; transmission of foreign Plasmodium vivax by Anopheles quadrimaculatus. Am J Trop Med Hyg 26, 477–483. [PubMed: 20996631]

16. Young MD, Eyles DE, Burgess RW, and Jeffery GM (1955). Experimental testing of the immunity of Negroes to Plasmodium vivax. J Parasitol 41, 315–318. [PubMed: 13252508]

17. Bray RS (1957). Plasmodium ovale in Liberia. Am J Trop Med Hyg 6, 961–970. 10.4269/ajtmh.1957.6.961. [PubMed: 13487966]

18. Bray RS (1958). The susceptibility of Liberians to the Madagascar strain of Plasmodium vivax. J Parasitol 44, 371–373. [PubMed: 13564349]

19. Miller LH, Mason SJ, Clyde DF, and McGinniss MH (1976). The resistance factor to Plasmodium vivax in blacks. The Duffy-blood-group genotype, FyFy. N Engl J Med 295, 302–304. 10.1056/NEJM197608052950602. [PubMed: 778616]

20. Chitnis CE, and Miller LH (1994). Identification of the erythrocyte binding domains of Plasmodium vivax and Plasmodium knowlesi proteins involved in erythrocyte invasion. J Exp Med 180, 497–506. 10.1084/jem.180.2.497. [PubMed: 8046329]

21. Batchelor JD, Malpede BM, Omattage NS, DeKoster GT, Henzler-Wildman KA, and Tolia NH (2014). Red blood cell invasion by Plasmodium vivax: structural basis for DBP engagement of DARC. PLoS Pathog 10, e1003869. 10.1371/journal.ppat.1003869.

22. Batchelor JD, Zahm JA, and Tolia NH (2011). Dimerization of Plasmodium vivax DBP is induced upon receptor binding and drives recognition of DARC. Nat Struct Mol Biol 18, 908–914. 10.1038/nsmb.2088. [PubMed: 21743458]

23. Chen E, Salinas ND, Huang Y, Ntumngia F, Plasencia MD, Gross ML, Adams JH, and Tolia NH (2016). Broadly neutralizing epitopes in the Plasmodium vivax vaccine candidate Duffy

Binding Protein. Proc Natl Acad Sci U S A 113, 6277–6282. 10.1073/pnas.1600488113. [PubMed: 27194724]

24. Carias LL, Dechavanne S, Nicolete VC, Sreng S, Suon S, Amaratunga C, Fairhurst RM, Dechavanne C, Barnes S, Witkowski B, et al. (2019). Identification and Characterization of Functional Human Monoclonal Antibodies to Plasmodium vivax Duffy-Binding Protein. J Immunol 202, 2648–2660. 10.4049/jimmunol.1801631. [PubMed: 30944159]
25. Urusova D, Carias L, Huang Y, Nicolete VC, Popovici J, Roesch C, Salinas ND, Dechavanne S, Witkowski B, Ferreira MU, et al. (2019). Structural basis for neutralization of Plasmodium vivax by naturally acquired human antibodies that target DBP. Nat Microbiol 4, 1486–1496. 10.1038/s41564-019-0461-2. [PubMed: 31133752]
26. Dickey TH, and Tolia NH (2023). Designing an effective malaria vaccine targeting Plasmodium vivax Duffy-binding protein. Trends Parasitol, S1471–4922(23)00147–2. 10.1016/j.pt.2023.06.011.
27. Tournamille C, Colin Y, Cartron JP, and Le Van Kim C (1995). Disruption of a GATA motif in the Duffy gene promoter abolishes erythroid gene expression in Duffy-negative individuals. Nat Genet 10, 224–228. 10.1038/ng0695-224. [PubMed: 7663520]
28. Zimmerman PA, Woolley I, Masinde GL, Miller SM, McNamara DT, Hazlett F, Mgone CS, Alpers MP, Genton B, Boatin BA, et al. (1999). Emergence of FY*A(null) in a Plasmodium vivax-endemic region of Papua New Guinea. Proc Natl Acad Sci U S A 96, 13973–13977. 10.1073/pnas.96.24.13973. [PubMed: 10570183]
29. Ranjan A, and Chitnis CE (1999). Mapping regions containing binding residues within functional domains of Plasmodium vivax and Plasmodium knowlesi erythrocyte-binding proteins. Proc Natl Acad Sci U S A 96, 14067–14072. 10.1073/pnas.96.24.14067. [PubMed: 10570199]
30. Aikawa M, Miller LH, Johnson J, and Rabbege J (1978). Erythrocyte entry by malarial parasites. A moving junction between erythrocyte and parasite. J Cell Biol 77, 72–82. 10.1083/jcb.77.1.72. [PubMed: 96121]
31. Zimmerman PA (2017). Plasmodium vivax Infection in Duffy-Negative People in Africa. Am J Trop Med Hyg 97, 636–638. 10.4269/ajtmh.17-0461. [PubMed: 28990906]
32. Twohig KA, Pfeffer DA, Baird JK, Price RN, Zimmerman PA, Hay SI, Gething PW, Battle KE, and Howes RE (2019). Growing evidence of Plasmodium vivax across malaria-endemic Africa. PLoS Negl Trop Dis 13, e0007140. 10.1371/journal.pntd.0007140.
33. Baird JK (2022). African Plasmodium vivax malaria improbably rare or benign. Trends in Parasitology 38, 683–696. 10.1016/j.pt.2022.05.006. [PubMed: 35667992]
34. Leong YW, Russell B, Malleret B, and Rénia L (2022). Erythrocyte tropism of malarial parasites: The reticulocyte appeal. Frontiers in Microbiology 13.
35. Woolley IJ, Hotmire KA, Sramkoski RM, Zimmerman PA, and Kazura JW (2000). Differential expression of the duffy antigen receptor for chemokines according to RBC age and FY genotype. Transfusion 40, 949–953. 10.1046/j.1537-2995.2000.40080949.x. [PubMed: 10960522]
36. Lopez GH, Condon JA, Wilson B, Martin JR, Liew Y-W, Flower RL, and Hyland CA (2015). A novel FY*A allele with the 265T and 298A SNPs formerly associated exclusively with the FY*B allele and weak Fy(b) antigen expression: implication for genotyping interpretative algorithms. Vox Sang 108, 52–57. 10.1111/vox.12185. [PubMed: 25092430]
37. Olsson ML, Smythe JS, Hansson C, Poole J, Mallinson G, Jones J, Avent ND, and Daniels G (1998). The Fy(x) phenotype is associated with a missense mutation in the Fy(b) allele predicting Arg89Cys in the Duffy glycoprotein. Br J Haematol 103, 1184–1191. 10.1046/j.1365-2141.1998.01083.x. [PubMed: 9886340]
38. Parasol N, Reid M, Rios M, Castilho L, Harari I, and Kosower NS (1998). A novel mutation in the coding sequence of the FY*B allele of the Duffy chemokine receptor gene is associated with an altered erythrocyte phenotype. Blood 92, 2237–2243. [PubMed: 9746760]
39. Tournamille C, Le Van Kim C, Gane P, Le Pennec PY, Roubinet F, Babinet J, Cartron JP, and Colin Y (1998). Arg89Cys substitution results in very low membrane expression of the Duffy antigen/receptor for chemokines in Fy(x) individuals. Blood 92, 2147–2156. [PubMed: 9731074]
40. Mallinson G, Soo KS, Schall TJ, Pisacka M, and Anstee DJ (1995). Mutations in the erythrocyte chemokine receptor (Duffy) gene: the molecular basis of the Fya/Fyb antigens and identification of

a deletion in the Duffy gene of an apparently healthy individual with the Fy(a-b-) phenotype. Br J Haematol 90, 823–829. 10.1111/j.1365-2141.1995.tb05202.x. [PubMed: 7669660]

41. Rios M, Chaudhuri A, Mallinson G, Sausais L, Gomensoro-Garcia AE, Hannon J, Rosenberger S, Poole J, Burgess G, Pogo O, et al. (2000). New genotypes in Fy(a-b-) individuals: nonsense mutations (Trp to stop) in the coding sequence of either FY A or FY B. Br J Haematol 108, 448–454. 10.1046/j.1365-2141.2000.01882.x. [PubMed: 10691880]
42. Wasniowska K, Blanchard D, Janvier D, Wang ZX, Peiper SC, Hadley TJ, and Lisowska E (1996). Identification of the Fy6 epitope recognized by two monoclonal antibodies in the N-terminal extracellular portion of the Duffy antigen receptor for chemokines. Mol Immunol 33, 917–923. 10.1016/s0161-5890(96)00056-9. [PubMed: 8960115]
43. Wasniowska K, Petit-LeRoux Y, Tournamille C, Le van Kim C, Cartron JP, Colin Y, Lisowska E, and Blanchard D (2002). Structural characterization of the epitope recognized by the new anti-Fy6 monoclonal antibody NaM 185–2C3. Transfus Med 12, 205–211. 10.1046/j.1365-3148.2002.00373.x. [PubMed: 12164140]
44. Smolarek D, Hattab C, Hassanzadeh-Ghassabeh G, Cochet S, Gutiérrez C, de Brevern AG, Udomsangpetch R, Picot J, Grodecka M, Wasniowska K, et al. (2010). A recombinant dromedary antibody fragment (VHH or nanobody) directed against human Duffy antigen receptor for chemokines. Cell Mol Life Sci 67, 3371–3387. 10.1007/s00018-010-0387-6. [PubMed: 20458517]
45. Smolarek D, Hattab C, Buczkowska A, Kaczmarek R, Jarząb A, Cochet S, de Brevern AG, Lukasiewicz J, Jachymek W, Niedziela T, et al. (2015). Studies of a murine monoclonal antibody directed against DARC: reappraisal of its specificity. PLoS One 10, e0116472. 10.1371/journal.pone.0116472.
46. King CL, Adams JH, Xianli J, Grimberg BT, McHenry AM, Greenberg LJ, Siddiqui A, Howes RE, da Silva-Nunes M, Ferreira MU, et al. (2011). Fy(a)/Fy(b) antigen polymorphism in human erythrocyte Duffy antigen affects susceptibility to Plasmodium vivax malaria. Proc Natl Acad Sci U S A 108, 20113–20118. 10.1073/pnas.1109621108. [PubMed: 22123959]
47. Tran TM, Moreno A, Yazdani SS, Chitnis CE, Barnwell JW, and Galinski MR (2005). Detection of a Plasmodium vivax erythrocyte binding protein by flow cytometry. Cytometry A 63, 59–66. 10.1002/cyto.a.20098. [PubMed: 15584018]
48. Haynes JD, Dalton JP, Klotz FW, McGinniss MH, Hadley TJ, Hudson DE, and Miller LH (1988). Receptor-like specificity of a Plasmodium knowlesi malarial protein that binds to Duffy antigen ligands on erythrocytes. J Exp Med 167, 1873–1881. 10.1084/jem.167.6.1873. [PubMed: 2838562]
49. Horuk R (2015). The Duffy Antigen Receptor for Chemokines DARC/ACKR1. Front Immunol 6, 279. 10.3389/fimmu.2015.00279. [PubMed: 26097477]
50. Miller LH, Hudson D, and Haynes JD (1988). Identification of Plasmodium knowlesi erythrocyte binding proteins. Mol Biochem Parasitol 31, 217–222. 10.1016/0166-6851(88)90151-x. [PubMed: 3221909]
51. Wertheimer SP, and Barnwell JW (1989). Plasmodium vivax interaction with the human Duffy blood group glycoprotein: identification of a parasite receptor-like protein. Exp Parasitol 69, 340–350. 10.1016/0014-4894(89)90083-0. [PubMed: 2680568]
52. Choe H, Moore MJ, Owens CM, Wright PL, Vasilieva N, Li W, Singh AP, Shakri R, Chitnis CE, and Farzan M (2005). Sulphated tyrosines mediate association of chemokines and Plasmodium vivax Duffy binding protein with the Duffy antigen/receptor for chemokines (DARC). Mol Microbiol 55, 1413–1422. 10.1111/j.1365-2958.2004.04478.x. [PubMed: 15720550]
53. Kitchen SF (1938). The Infection of Reticulocytes by Plasmodium Vivax. The American Journal of Tropical Medicine and Hygiene s1–18, 347–359. 10.4269/ajtmh.1938.s1-18.347.
54. Mons B (1990). Preferential invasion of malarial merozoites into young red blood cells. Blood Cells 16, 299–312. [PubMed: 2257316]
55. Russell B, Suwanarusk R, Borlon C, Costa FTM, Chu CS, Rijken MJ, Sriprawat K, Warter L, Koh EGL, Malleret B, et al. (2011). A reliable ex vivo invasion assay of human reticulocytes by Plasmodium vivax. Blood 118, e74–81. 10.1182/blood-2011-04-348748. [PubMed: 21768300]

56. Lim C, Pereira L, Saliba KS, Mascarenhas A, Maki JN, Chery L, Gomes E, Rathod PK, and Duraisingh MT (2016). Reticulocyte Preference and Stage Development of Plasmodium vivax Isolates. J Infect Dis 214, 1081–1084. 10.1093/infdis/jiw303. [PubMed: 27432121]
57. Cho J-S, Russell B, Kosaisavee V, Zhang R, Colin Y, Bertrand O, Chandramohanadas R, Chu CS, Nosten F, Renia L, et al. (2016). Unambiguous determination of Plasmodium vivax reticulocyte invasion by flow cytometry. Int J Parasitol 46, 31–39. 10.1016/j.ijpara.2015.08.003. [PubMed: 26385436]
58. Ovchynnikova E, Aglialoro F, Bentlage AEH, Vidarsson G, Salinas ND, von Lindern M, Tolia NH, and van den Akker E (2017). DARC extracellular domain remodeling in maturating reticulocytes explains Plasmodium vivax tropism. Blood 130, 1441–1444. 10.1182/blood-2017-03-774364. [PubMed: 28754683]
59. Malleret B, Li A, Zhang R, Tan KSW, Suwanarusk R, Claser C, Cho JS, Koh EGL, Chu CS, Pukrittayakamee S, et al. (2015). Plasmodium vivax: restricted tropism and rapid remodeling of CD71-positive reticulocytes. Blood 125, 1314–1324. 10.1182/blood-2014-08-596015. [PubMed: 25414440]
60. Gruszczyk J, Kanjee U, Chan L-J, Menant S, Malleret B, Lim NTY, Schmidt CQ, Mok Y-F, Lin K-M, Pearson RD, et al. (2018). Transferrin receptor 1 is a reticulocyte-specific receptor for Plasmodium vivax. Science 359, 48–55. 10.1126/science.aan1078. [PubMed: 29302006]
61. Garnham PCC (1966). Malaria parasites and other haemosporidia (Blackwell Scientific).
62. Duchene J, Novitzky-Basso I, Thiriot A, Casanova-Acebes M, Bianchini M, Etheridge SL, Hub E, Nitz K, Artinger K, Eller K, et al. (2017). Atypical chemokine receptor 1 on nucleated erythroid cells regulates hematopoiesis. Nat Immunol 18, 753–761. 10.1038/ni.3763. [PubMed: 28553950]
63. Hu J, Liu J, Xue F, Halverson G, Reid M, Guo A, Chen L, Raza A, Galili N, Jaffray J, et al. (2013). Isolation and functional characterization of human erythroblasts at distinct stages: implications for understanding of normal and disordered erythropoiesis in vivo. Blood 121, 3246–3253. 10.1182/blood-2013-01-476390. [PubMed: 23422750]
64. Kondo M, Wagers AJ, Manz MG, Prohaska SS, Scherer DC, Beilhack GF, Shizuru JA, and Weissman IL (2003). Biology of hematopoietic stem cells and progenitors: implications for clinical application. Annu Rev Immunol 21, 759–806. 10.1146/annurev.immunol.21.120601.141007. [PubMed: 12615892]
65. Attar A (2014). Changes in the Cell Surface Markers During Normal Hematopoiesis: A Guide to Cell Isolation. In Global Journal of Hematology and Blood Transfusion, pp. 20–28. 10.15379/2408-9877.2014.01.01.4.
66. Sidney LE, Branch MJ, Dunphy SE, Dua HS, and Hopkinson A (2014). Concise review: evidence for CD34 as a common marker for diverse progenitors. Stem Cells 32, 1380–1389. 10.1002/stem.1661. [PubMed: 24497003]
67. Mori Y, Chen JY, Pluvinage JV, Seita J, and Weissman IL (2015). Prospective isolation of human erythroid lineage-committed progenitors. Proc Natl Acad Sci U S A 112, 9638–9643. 10.1073/pnas.1512076112. [PubMed: 26195758]
68. Machherndl-Spandl S, Suessner S, Danzer M, Proell J, Gabriel C, Lauf J, Sylie R, Klein H-U, Béné MC, Weltermann A, et al. (2013). Molecular pathways of early CD105-positive erythroid cells as compared with CD34-positive common precursor cells by flow cytometric cell-sorting and gene expression profiling. Blood Cancer J 3, e100. 10.1038/bcj.2012.45. [PubMed: 23310930]
69. Wangen JR, Eidenschink Brodersen L, Stolk TT, Wells DA, and Loken MR (2014). Assessment of normal erythropoiesis by flow cytometry: important considerations for specimen preparation. Int J Lab Hematol 36, 184–196. 10.1111/ijlh.12151. [PubMed: 24118926]
70. Kono M, Kondo T, Takagi Y, Wada A, and Fujimoto K (2009). Morphological definition of CD71 positive reticulocytes by various staining techniques and electron microscopy compared to reticulocytes detected by an automated hematology analyzer. Clin Chim Acta 404, 105–110. 10.1016/j.cca.2009.03.017. [PubMed: 19302987]
71. Menard D, Barnadas C, Bouchier C, Henry-Halldin C, Gray LR, Ratsimbasoa A, Thonier V, Carod J-F, Domarle O, Colin Y, et al. (2010). Plasmodium vivax clinical malaria is commonly observed in Duffy-negative Malagasy people. Proc Natl Acad Sci U S A 107, 5967–5971. 10.1073/pnas.0912496107. [PubMed: 20231434]

72. Howes RE, Franchard T, Rakotomanga TA, Ramiranirina B, Zikursh M, Cramer EY, Tisch DJ, Kang SY, Ramboarina S, Ratsimbasoa A, et al. (2018). Risk Factors for Malaria Infection in Central Madagascar: Insights from a Cross-Sectional Population Survey. Am J Trop Med Hyg 99, 995–1002. 10.4269/ajtmh.18-0417. [PubMed: 30182923]
73. Oboh MA, Singh US, Ndiaye D, Badiane AS, Ali NA, Bharti PK, and Das A (2020). Presence of additional Plasmodium vivax malaria in Duffy negative individuals from Southwestern Nigeria. Malar J 19, 229. 10.1186/s12936-020-03301-w. [PubMed: 32590997]
74. Obaldia N, Meibalan E, Sa JM, Ma S, Clark MA, Mejia P, Moraes Barros RR, Otero W, Ferreira MU, Mitchell JR, et al. (2018). Bone Marrow Is a Major Parasite Reservoir in Plasmodium vivax Infection. mBio 9, e00625–18. 10.1128/mBio.00625-18. [PubMed: 29739900]
75. Kho S, Qotrunnada L, Leonardo L, Andries B, Wardani PAI, Fricot A, Henry B, Hardy D, Margyaningsih NI, Apriyanti D, et al. (2021). Evaluation of splenic accumulation and colocalization of immature reticulocytes and Plasmodium vivax in asymptomatic malaria: A prospective human splenectomy study. PLoS Med 18, e1003632. 10.1371/journal.pmed.1003632.
76. Kho S, Qotrunnada L, Leonardo L, Andries B, Wardani PAI, Fricot A, Henry B, Hardy D, Margyaningsih NI, Apriyanti D, et al. (2021). Hidden Biomass of Intact Malaria Parasites in the Human Spleen. N Engl J Med 384, 2067–2069. 10.1056/NEJMc2023884. [PubMed: 34042394]
77. Cenariu D, Iluta S, Zimta A-A, Petrushev B, Qian L, Dirzu N, Tomuleasa C, Bumbea H, and Zaharie F (2021). Extramedullary Hematopoiesis of the Liver and Spleen. Journal of Clinical Medicine 10, 5831. 10.3390/jcm10245831. [PubMed: 34945127]
78. Malleret B, El Sahili A, Tay MZ, Carissimo G, Ong ASM, Novera W, Lin J, Suwanarusk R, Kosaisavee V, Chu TTT, et al. (2021). Plasmodium vivax binds host CD98hc (SLC3A2) to enter immature red blood cells. Nat Microbiol 6, 991–999. 10.1038/s41564-021-00939-3. [PubMed: 34294905]
79. Ferreira R, Ohneda K, Yamamoto M, and Philipsen S (2005). GATA1 function, a paradigm for transcription factors in hematopoiesis. Mol Cell Biol 25, 1215–1227. 10.1128/MCB.25.4.1215-1227.2005. [PubMed: 15684376]
80. Fernandez-Becerra C, Lelievre J, Ferrer M, Anton N, Thomson R, Peligero C, Almela MJ, Lacerda MV, Herreros E, and Del Portillo HA (2013). Red blood cells derived from peripheral blood and bone marrow $CD34^{+}$ human haematopoietic stem cells are permissive to Plasmodium parasites infection. Mem Inst Oswaldo Cruz 108, 801–803. 10.1590/0074-0276108062013019. [PubMed: 24037205]
81. Thomson-Luque R, and Bautista JM (2021). Home Sweet Home: Plasmodium vivax-Infected Reticulocytes-The Younger the Better? Front Cell Infect Microbiol 11, 675156. 10.3389/fcimb.2021.675156. [PubMed: 34055670]
82. Aitken GJ (1943). Sternal puncture in the diagnosis of malaria. The Lancet 242, 466–468. 10.1016/S0140-6736(00)87486-3.
83. Lacerda M.V.G. de, Hipólito JR, and Passos L.N. da M. (2008). Chronic Plasmodium vivax infection in a patient with splenomegaly and severe thrombocytopenia. Rev Soc Bras Med Trop 41, 522–523. 10.1590/s0037-86822008000500021. [PubMed: 19009202]
84. Brito MAM, Baro B, Raiol TC, Ayllon-Hermida A, Safe IP, Deroost K, Figueiredo EFG, Costa AG, Armengol MDP, Sumoy L, et al. (2022). Morphological and Transcriptional Changes in Human Bone Marrow During Natural Plasmodium vivax Malaria Infections. J Infect Dis 225, 1274–1283. 10.1093/infdis/jiaa177. [PubMed: 32556188]
85. Wickramarachchi T, Devi YS, Mohmmed A, and Chauhan VS (2008). Identification and characterization of a novel Plasmodium falciparum merozoite apical protein involved in erythrocyte binding and invasion. PLoS One 3, e1732. 10.1371/journal.pone.0001732. [PubMed: 18320051]
86. Rastogi N, and Rehman N (2018). Changes in bone marrow in malaria-a prospective study of 47 cases. International Journal of Research in Medical Sciences 6, 232–235. 10.18203/2320-6012.ijrms20175725.
87. Jandial R, Bhagat R, and Kumar V (2019). Different Causes of Pyrexia of Unknown Origin on Bone Marrow Examination- An Institutional Experience. jmscr 7. 10.18535/jmscr/v7i7.93.

88. Silva-Filho JL, Dos-Santos JC, Judice C, Beraldi D, Venugopal K, Lima D, Nakaya HI, De Paula EV, Lopes SC, Lacerda MV, et al. (2021). Total parasite biomass but not peripheral parasitaemia is associated with endothelial and haematological perturbations in Plasmodium vivax patients. Elife 10, e71351. 10.7554/eLife.71351. [PubMed: 34585667]

89. Barber BE, William T, Grigg MJ, Parameswaran U, Piera KA, Price RN, Yeo TW, and Anstey NM (2015). Parasite biomass-related inflammation, endothelial activation, microvascular dysfunction and disease severity in vivax malaria. PLoS Pathog. 11, e1004558. 10.1371/journal.ppat.1004558.

90. Habib I, Smolarek D, Hattab C, Grodecka M, Hassanzadeh-Ghassabeh G, Muyldermans S, Sagan S, Gutiérrez C, Laperche S, Le-Van-Kim C, et al. (2013). V(H)H (nanobody) directed against human glycophorin A: a tool for autologous red cell agglutination assays. Anal Biochem 438, 82–89. 10.1016/j.ab.2013.03.020. [PubMed: 23541519]

91. Tournamille C, Blancher A, Le Van Kim C, Gane P, Apoil PA, Nakamoto W, Cartron JP, and Colin Y (2004). Sequence, evolution and ligand binding properties of mammalian Duffy antigen/receptor for chemokines. Immunogenetics 55, 682–694. 10.1007/s00251-003-0633-2. [PubMed: 14712331]

92. Chaudhuri A, Zbrzezna V, Polyakova J, Pogo AO, Hesselgesser J, and Horuk R (1994). Expression of the Duffy antigen in K562 cells. Evidence that it is the human erythrocyte chemokine receptor. J Biol Chem 269, 7835–7838. [PubMed: 8132497]

93. Roobsoong W (2015). The In Vitro Invasion Inhibition Assay (IIA) for Plasmodium vivax. In Malaria Vaccines: Methods and Protocols Methods in Molecular Biology., Vaughan A, ed. (Springer), pp. 187–196. 10.1007/978-1-4939-2815-6_15.

Highlights

- Duffy blood group protein (Fy) is naturally expressed on Fy-negative red blood cells.
- Fy expression is higher on erythroid precursors than on red blood cells.
- Fy protein is expressed in early erythropoietic stages in Fy-negative individuals.
- *P. vivax* invades Fy-positive and Fy-negative erythroid cells *in vitro*.

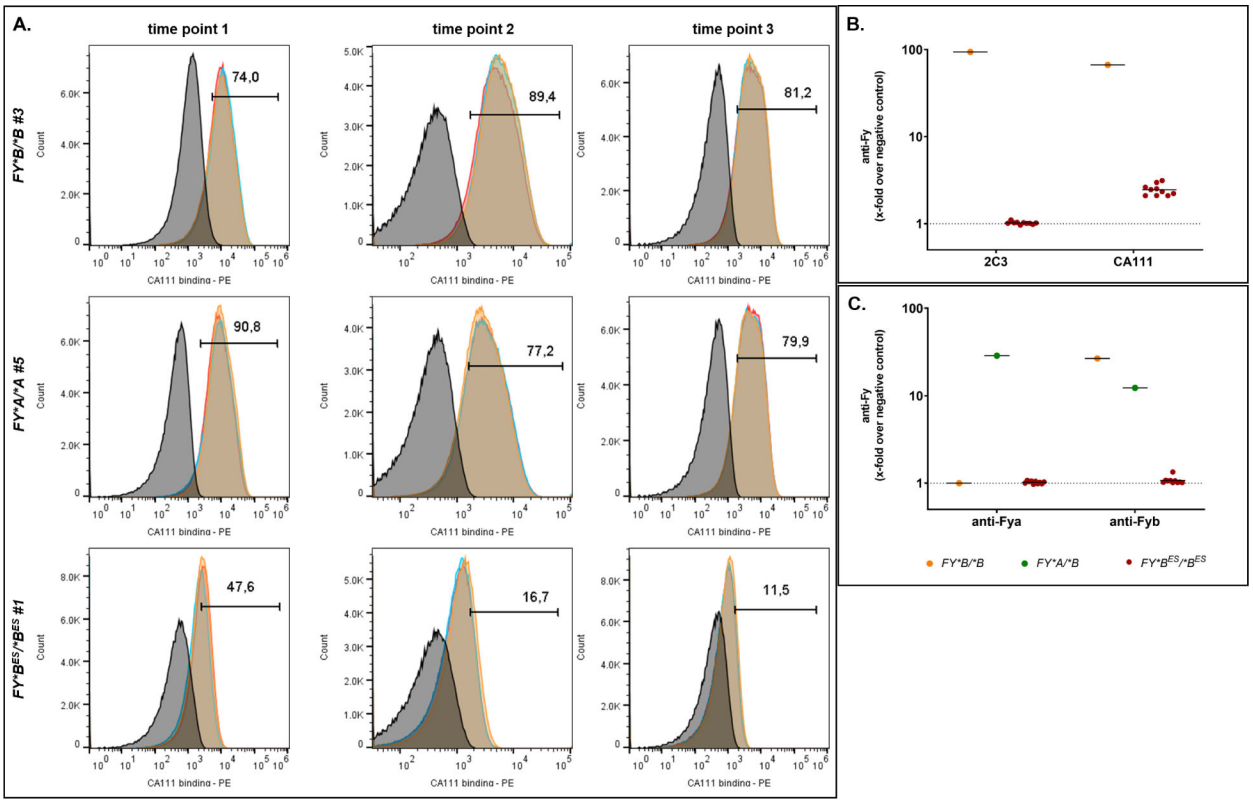

Figure 1. Binding of Fy-specific antibodies on Fy-positive and Fy-negative pbRBC.

A - Direct binding of CA111 anti-Fy6 to pbRBC from *FY*B/*B*, *FY*A/*A* and *FY*B^{ES}/*B^{ES}* donors. Experiments were performed in triplicate (histograms in red, orange and blue in overlay) ; each donor was tested at three independent time points. Individual donor samples minus CA111 (plus anti-HA mouse antibody and goat anti-mouse PE-conjugated antibody) served as negative controls represented in each histogram in dark. The percentage of cells with CA111 binding (PE: phycoerythrin) over the background is indicated above the gate. The x-folds over negative control (geometric mean of fluorescence intensity (gmfi)) were higher than 48 for *FY*B/*B* #3 or *FY*A/*A* #5 and were equal to 6, 5 and 4 for *FY*B^{ES}/*B^{ES}* #1 at the three time points respectively.

B - Binding of 2C3 and CA111 anti-Fy6 to pbRBC from 1 *FY*B/*B* donor (orange) and 10 *FY*B^{ES}/*B^{ES}* donors (red). Each individual served as its own negative control: no primary antibody, only secondary antibodies (anti-HA (CA111), anti-mouse (2C3)). The x-fold is calculated using the gmfi of the binding of antibodies targeting the Fy6 epitope divided by the gmfi of the binding of the secondary antibody only.

C - Binding of anti-Fya and anti-Fyb to pbRBC from 1 *FY*A/*B* (green), 1 *FY*B/*B* donor (orange) and 10 *FY*B^{ES}/*B^{ES}* donors (red). Each individual served as its own negative control: no primary antibody, only secondary antibodies (anti-human-Fya or -Fyb). The x-fold is calculated using the gmfi of the binding of antibodies targeting the Fy epitope divided by the gmfi of the binding of the secondary antibody only.

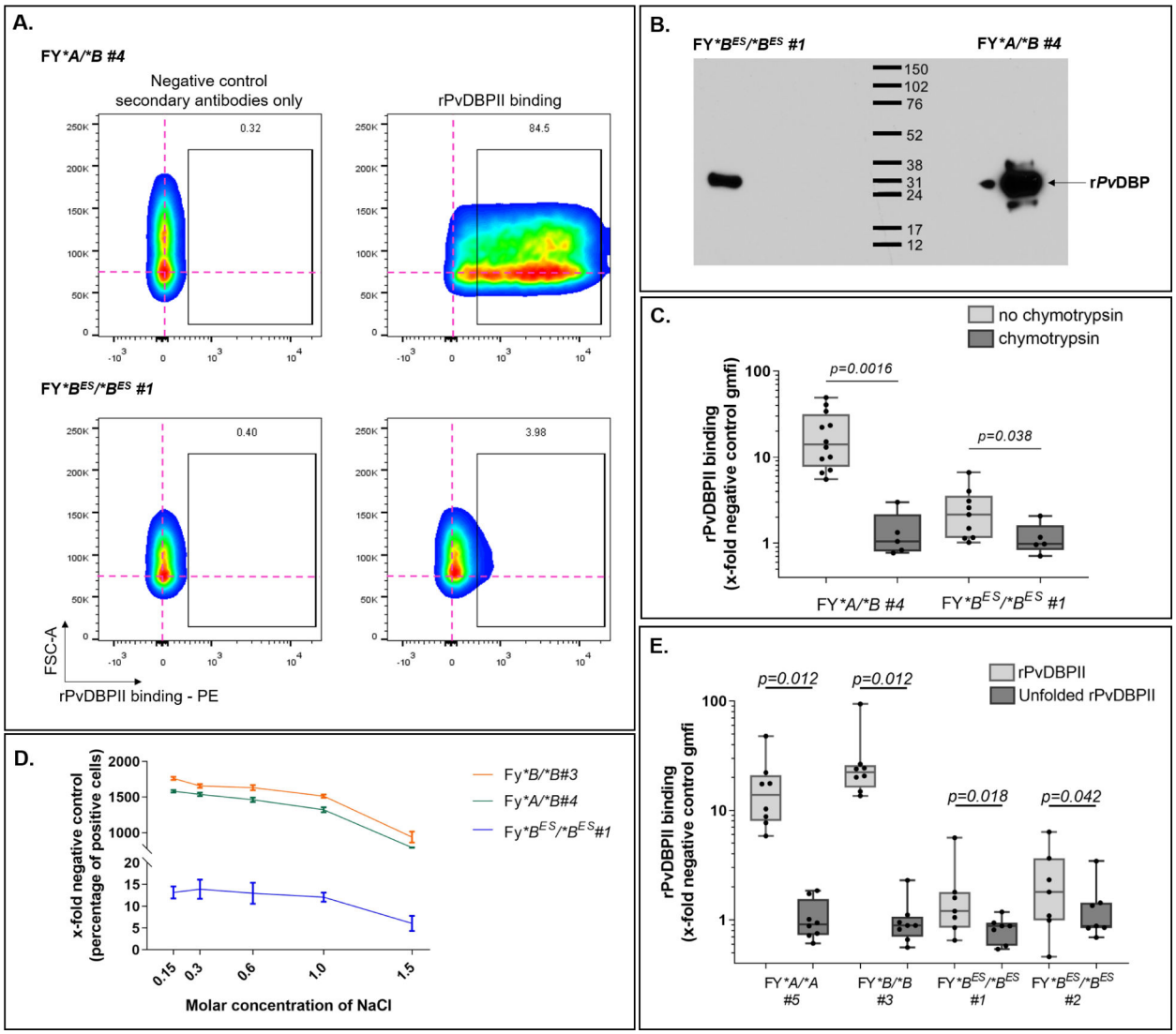

Figure 2. rPvDBPII binding on *FY*B^ES /*B^ES* pbRBC.

A - rPvDBPII binding on *FY*A /*B* and *FY*B^ES /*B^ES* pbRBC. The pink cross provides a point of reference for cell populations in negative controls (no rPvDBPII and secondary antibody only). The percentage of rPvDBPII binding cells over background is indicated above the gate.

B - rPvDBPII binding and dissociation to Fy-positive and Fy-negative pbRBC - pbRBC were exposed to rPvDBPII (20 μg/mL, 2 hr.; room temperature) to allow protein binding. The western blot of dissociated proteins from *FY*B^ES/*B^ES* (left) and *FY*A/*B* (right) pbRBC was probed with a polyclonal anti-PvDBP. The western blot included here is from an original intact gel and blot. This experiment was repeated 3 more times on fresh RBC from 2 *FY*B^ES/*B^ES* donors (data not shown). Those data were complemented with flow cytometry data.

C - Chymotrypsin binding assessment - Without chymotrypsin treatment (light gray boxes); with chymotrypsin treatment (dark gray boxes); individual data points (filled black circles); *FY*A/*B* - without chymotrypsin (N=12); with chymotrypsin (N=5); for *FY*B^ES/*B^ES* -

without chymotrypsin (N=9); with chymotrypsin (N=5); evaluated by non-parametric paired Wilcoxon rank-sum test. *FY*A/*B* (*P-value* = 0.0016); *FY*B^{ES}/*B^{ES}* (*P-value* = 0.038).

D - rPvDBPII dissociation assessment of non-specific binding - No significant reduction in rPvDBPII binding was observed across increasing NaCl concentrations from 0.15M to 1.0M; addition of 1.5M NaCl caused significant reduction in rPvDBPII binding (Pearson Chi^2 test, p=0.014: Pearson Chi^2=6.0). Each curve represents a different donor: *FY*B/*B #3* (black circle), *FY*A/*B #4* (white square), *FY*B^{ES}/*B^{ES} #1* (black triangle).

E - Comparative binding between folded (gray boxes) and unfolded rPvDBPII (dark boxes; same amino acid sequence) to pbRBC - Non-parametric Wilcoxon matched pairs sign rank test evaluated the median differences between rPvDBPII folded vs unfolded; n=8 for each Fy-positive and n=7 for each Fy-negative donors. *FY*A/*A*: p=0.012; *FY*B/*B*: p=0.012; *FY*B^{ES}/*B^{ES}* #1: p=0.018; *FY*B^{ES}/*B^{ES}* #2: p=0.042. Unfolded rPvDBPII interaction with pbRBC from four study participants showed no significant difference (non-parametric median test Pearson Chi^2: p=0.853).

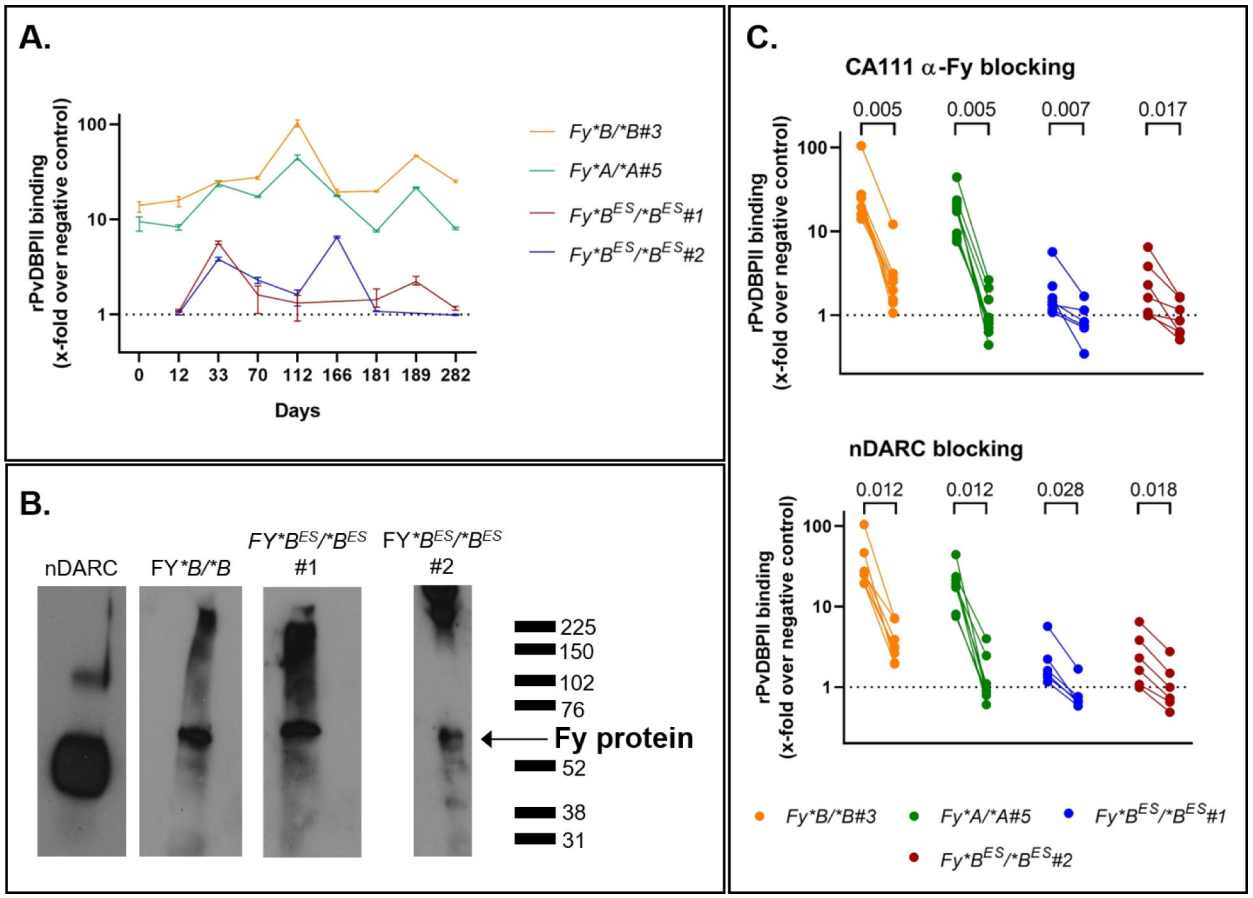

Figure 3. Specific rPvDBPII binding on Fy-positive and Fy-negative pbRBC over time.

A - rPvDBPII binding on Fy-positive and Fy-negative pbRBC over time – Binding of rPvDBPII to pbRBC was followed for up to 282 days (10 months): one *FY*B/*B* (donor #3, orange), one *FY*A/*A* (donor #5, green), two *FY*B*^{ES}*/*B*^{ES} (donor #1, red; donor #2, blue); binding tested in triplicate (minimum, maximum and mean value) and represented as the x-fold increase over negative control. Those data complete the Fy-expression in the cross sectional study represented in Fig1B. Each donor served as its negative control for each time point. The same antibodies and flow cytometer (Attune NxT) were used in each experiment.

B - Specific capture and detection of the Fy protein from the surface of pbRBC.

This figure presents direct evidence of the specific capture, immunoprecipitation and detection of the Fy protein from the surface of the pbRBC of *FY*B/*B* and *FY*B*^{ES}*/*B*^{ES} donors. In the left panel, nDARCIg panel – the monomeric and dimeric nDARCIg species were distinguishable. Experimental panels – Fy6-specific CA111-based capture of the Fy protein from pbRBC of *FY*B/*B* (Donor #3; day 112), *FY*B*^{ES}*/*B*^{ES} (Donor #1; day 112) and *FY*B*^{ES}*/*B*^{ES} (Donor #2; day 189). Western blot detection of CA111-captured Fy protein was performed using polyclonal anti-ACKR1 (LS Bioscience). **See** SI Methods Section 7 **for western blot raw data**. This experiment was repeated twice on fresh RBC from 2 *FY*B*^{ES}*/*B*^{ES} donors (data not shown). Those data were complemented with flow cytometry data.

C - Blocking of the rPvDBPII binding to Fy-positive and Fy-negative pbRBC – Upper Panel – Inhibition of rPvDBPII binding with addition of the anti-Fy6-specific CA111. Lower Panel – Inhibition of rPvDBPII binding with addition of the nDARCIg. Only the experiments showing a decrease of at least two times were represented on the graphics. Experiments included in the statistical analysis: n=9 for *FY*B/*B#3*, n=7 for *FY*A/*A#5*, n=7 for $FY*B^{ES}/*B^{ES}$#1, n=7 for $FY*B^{ES}/*B^{ES}$#2 - Non-parametric Wilcoxon matched pairs sign rank test evaluated the differences of rPvDBPII binding without or with blocking for each individual. The dashed line represents equivalent binding compared to the negative controls. Each dot is the mean of 2 to 3 technical replicates. Data of rPvDBPII binding in Fig3C are also represented in Fig3A with error bars. Two connected dots refer to one experiment.

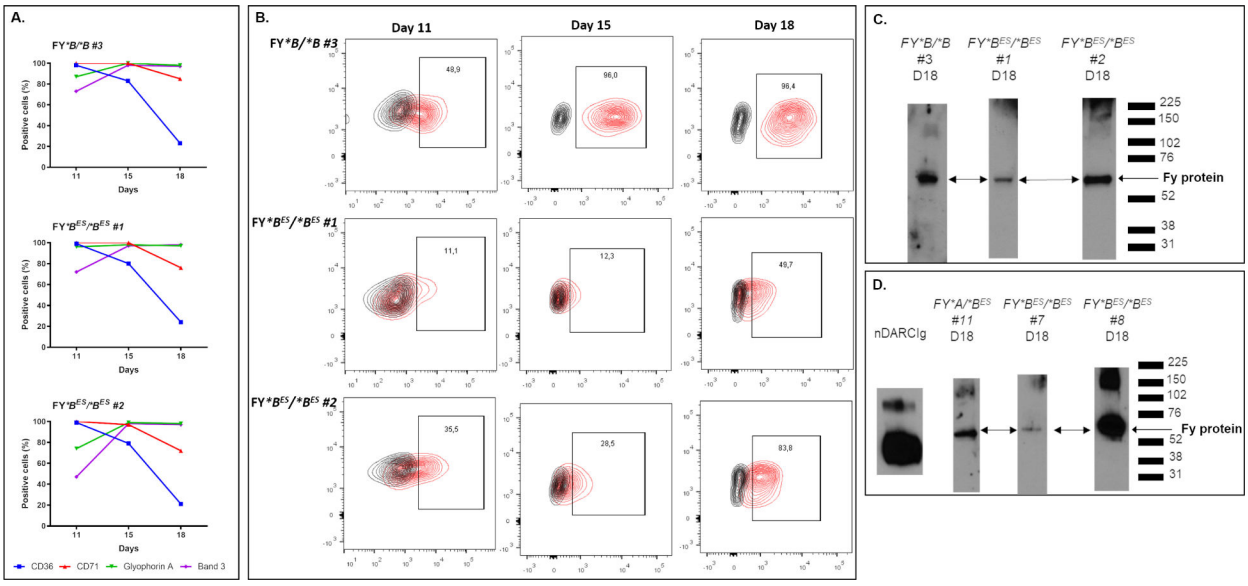

Figure 4. Fy protein expression during *in vitro* CD34^{pos} erythroid precursors differentiation.

The CD34^{pos} erythroid precursor cells were expanded and differentiated for over 21 days.

A - Monitoring of CD34 positive cells differentiation *in vitro*. CD34^{pos} erythroid precursor cells were collected from the peripheral blood of 3 donors (1 Fy-positive and 2 Fy-negatives). *In vitro* differentiation was monitored by the presence/absence of the surface markers CD36, CD71, Glycophorin A and Band 3 on CD34^{pos} erythroid precursor cells. As expected, during the differentiation process, the cells were losing the CD36 and CD71 signals whereas Glycophorin A and Band 3 signals were increasing. Overall, the cells from all the donors were observed to be at comparable stages over time.

B - Fy expression on differentiated CD34^{pos} from *FY*B/*B* and *FY*B^{ES}/*B^{ES}* donors. At Day11, Day15 and Day18, the expression of Fy protein was detected by flow cytometry using CA111 anti-Fy6. For each donor, the percentage of positive cells for the binding of CA111 is annotated in the black box (population in red within the CA111-PE positive gate) in comparison to its negative control (population in black, e.g. secondary antibody only). mfi: mean of fluorescence intensity.

C, D - Expression of Fy protein in erythroid precursors isolated from peripheral blood of *FY*B/*B* and *FY*B^{ES}/*B^{ES}* donors (**C**) and from bone marrow of *FY*A/*B^{ES}* and *FY*B^{ES}/*B^{ES}* donors (**D**). Differentiated cells were harvested on Day18, membrane proteins were extracted and immunoprecipitated with CA111 anti-Fy6. The protein captured by Fy-specific CA111 were detected with a commercial polyclonal anti-ACKR1 antibody by western blot. All original western blots and re-organization of lanes to present salient results are described SI Methods Section 7. The experiments of the Fig4C were repeated at Day11 and Day18 on differentiated CD34^{pos} from two FY*B^{ES}/*B^{ES} donors (data not shown). The experiments of the Fig4D were repeated at Day11 and Day15 on differentiated CD34^{pos} from two FY*B^{ES}/*B^{ES} donors and Day15 on differentiated CD34^{pos} from one other FY*B^{ES}/*B^{ES} donor (data not shown). Those data were complemented with flow cytometry data.

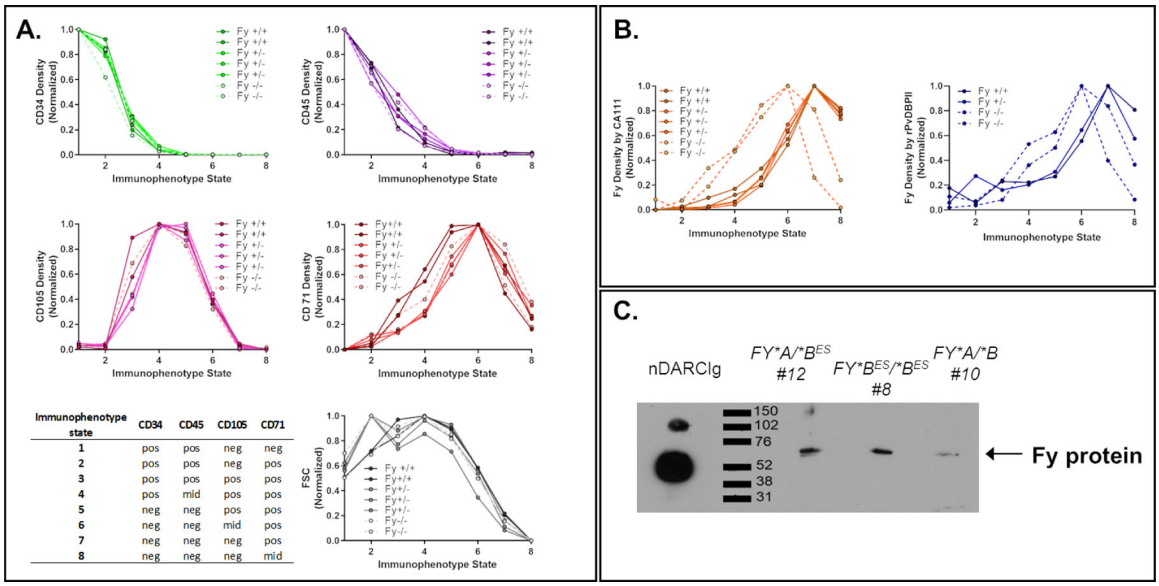

Figure 5. ***Ex vivo*** **expression of Fy protein among erythroid precursor sub-populations from bone marrow aspirates.**

A, B - In the bone marrow, all stages of erythroid precursors are present except mature erythrocyte (that are circulating in the peripheral blood). The gating strategy is detailed in the SI and summarized in the table up left (pos: positive, mid: middle, neg: no expression). The density (mean of fluorescence intensity divided by the size of the cells) of each CD markers as well as CA111 anti-Fy6 or rPvDBPII binding to Fy protein was represented in different graphics. The Fy-negative donors were represented in dashed lines in the graphics. The profile of CD marker expression was similar between all Fy genotypes (**A**) whereas Fy expression appeared to be earlier during erythropoiesis in Fy negative compare to Fy positive individuals (**B**).

C - Expression of Fy protein in $Fy*B^{ES}/*B^{ES}$ CD45 negative erythroid precursors from *ex vivo* bone marrow. CD45 negative cells (erythroid precursors in bone marrow) of three bone marrow samples were sorted by flow cytometry. The membrane proteins of the sorted cells were then immunoprecipitated with the CA111 anti-Fy6 and revealed by Western blot with a commercial polyclonal anti-ACKR1 antibody (arrow). Fy-positive and Fy-negative showed a signal for the Fy protein in erythroid precursors. The western blot included here is from an original intact gel and blot. **See** SI Methods Section 7 **for western blot raw data**. This experiment was complemented with flow cytometry data.

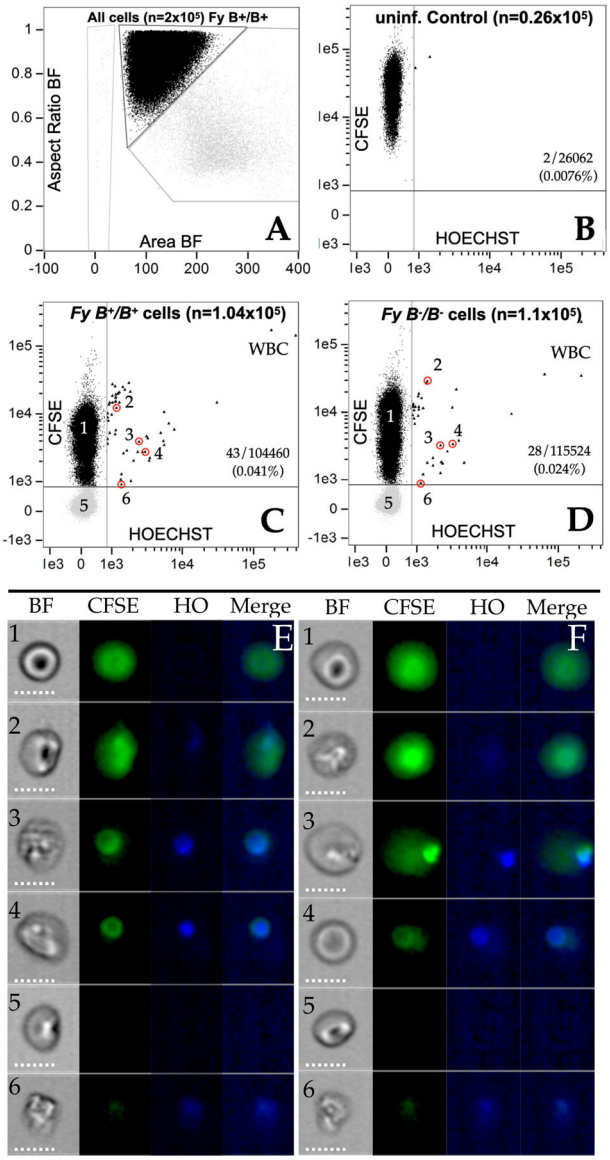

Figure 6. *In vitro* invasion of pbRBCs from Fy-positive and Fy-negative North Americans by Malagasy *P. vivax* isolate.

6A. single cells (black data points) versus multiple (gray data points) cells by aspect ratio and area in the brightfield image; **6B**; Control image using uninfected cells previously stained with CFSE. Y-axis CFSE; X-axis Hoechst; **6C**. AMP2016.14 (CFSE[-]) mixed with Fy-positive, *FY*B/*B* target cells (CFSE[+]); **6D**. AMP2016.14 (CFSE[-]) mixed with Fy-negative, $FY*B^{ES}/*B^{ES}$ target cells (CFSE[+]); **8E1- E6.** Individual cells identified in Panel 6C from AMP2016.14 added to *FY*B/*B* (Fy-positive). **8F1- F6.** Individual cells identified in Panel 6D from AMP2016.14 added to $FY*B^{ES}/*B^{ES}$ (Fy-negative). Additional data and plots are provided in the SI (Figure S8, Table S2, Figure S9, Figure S10, Figure S11).

KEY RESOURCES TABLE

REAGENT or RESOURCE	SOURCE	IDENTIFIER
Recombinant proteins		
rPvDBPII	Gift from Dr. Niraj Tolia	https://doi.org/10.1038/nsmb.2088
unfolded rPcDBPII	Material produced at CWRU	https://doi.org/10.1038/nsmb.2089
nDARCIg	Construct is a gift from Chetin Chitnis, material produced at CWRU	https://doi.org/10.1371/journal.pmed.0040337
rCXCR2	NovusBio	H00003579-P01
Antibodies		
conventional mouse 2C3 anti-Fy6	Gift from Dr. Yves Colin	https://doi.org/10.1046/j.1365-2141.2003.04533.x
single domain camelid CA111 (HA tag) anti-Fy6	Gift from Dr. Olivier Bertrand and Dr. Yves Colin	https://doi.org/10.1007/s00018-010-0387-6
Anti-ACKR1 / DARC Antibody (aa1-63)	LS Biosciences	LS-C371451
HRP anti rabbit antibody	Milipore	AP187P
Mouse Anti-HA (IgG1)	Bioloegend	901502
Goat anti-mouse PE	eBioscience	12-4010-82
Goat anti-mouse APC	BD Biosciences	550826
Polyclonal rabbit anti-PvDBP (Rabbit 2)		https://doi.org/10.1371/journal.pmed.0040337
Goat anti-rabbit APC	Invitrogen	31984
Goat anti-rabbit PE	Sigma	P9537
CD45 MicroBeads, human	Miltenyi	130-045-801
anti-CXCR2	R&D system	MAB331
Anti-Fy a (FY1)	Biorad	808-186
Anti-Fyb (FY2)	BioRad	808-191
anti-GlycoA PE-Cy7	BD Biosciences	563666
anti-CD36 APC	BD Biosciences	550956
anti-Band3-PE	American Research Product	IBGRL-BRIC6-PE
anti-CD71 APC	BD Biosciences	551374
anti-CD105 PE-Cy7	BD Biosciences	568753
anti-CD71 FITC	BD Biosciences	555536
anti-CD34 BV421	BD Biosciences	562577
anti-CD45 APC-Cy7	BD Biosciences	557833
anti-CD71 BV786	BD Biosciences	563768
mouse anti-HA tag	Miltenyi	130-098-404
mouse anti-His tag	Qiagen	34650
mouse anti-PE	Invitrogen	12-4010-82
mouse anti-PE	Jackson ImmunoResearch	115-115-164
Immunoprecipitation		
Protease inhibitor	Sigma Aldrich	4693159001 ; P8849
Dynabeads M-270 Carboxylic Acid	Invitrogen	14305D ; 10003D

REAGENT or RESOURCE	SOURCE	IDENTIFIER
EDC 1-(3-Dimethylaminopropyl)-3-ethylcarbodiimide hydrochloride	ACROS organics	171440010
Trypsin	Sigma Aldrich	T6567
IgG Elution Buffer	Thermo	21004
Neutralizing buffer 1 M tris Base pH 9 10X	Sigma Aldrich	1083820100
Western Blot		
Amersham standard autoradiography cassette, 24 × 30 cm	Dutscher	RPN11643
Amersham Hyperfilm™ ECL	Dustcher	28-9068-37
Mini-P Tetra Cell,2precast gel	Biorad	1658005
Dithiothreitol (DTT), 5 g	Biorad	1610611
Mini-PROTEAN TGX,4–20%,30µl 10 well,10	Biorad	4561093
Precision Plus Protein All Blue Standards, 500microliter, 50 applications	Biorad	1610373
Immun-Blot PVDF Membranes, 7 × 8.4 cm, 10	Biorad	1620174
Clarity Max ECL substrate,100ml	Biorad	1705062
Surebeads Protein G Magnetic Beads 3 ml	Biorad	1614023
Surebeads Magnetic Rack, 16 tube Holder	Biorad	1614916
Tris, 500 g	Biorad	1610716
Glycine, 1kg	Biorad	1610718
SDS, 100 g	Biorad	1610301
Bio-Safe Coomassie Stain, 1 L	Biorad	1610786
CD34+ Maturation		
CD34 MicroBead Kit	Miltenyi	130-046-702
holotransferrine	Sigma Aldrich	T0665 100mg
Human insulin	Sigma Aldrich	I9278 5ml
heparin	Sigma Aldrich	2106-10VL
AB serum	Sigma Aldrich	H4522-100ML
Hydrocortisone (dexamethasone)	Sigma Aldrich	D4902-25MG
Stem Cell Factor (SCF)	Peprotech	300-07
IL3	Peprotech	100-64
EPO	Peprotech	200-03
IMDM + glutamax	Gibco Thermo Fisher Scientific	31980030
Others		
Chymotrypsin	Roche Diagnostic	11418467001
Bovine Serum Albumin Fraction V	Sigma Aldrich	810531
Ficoll paque plus	Sigma Aldrich	GE17-1440-02
Nycodenz	MP Biomedicals	157750
Primers		
Duffy forward	Sigma Aldrich	5′-CAGGCAGTGGGCGTGGG-3′

REAGENT or RESOURCE	SOURCE	IDENTIFIER
Duffy reverse	Sigma Aldrich	5′-CTGCTAGCTAGGATACCCAG-3′
FY*B/FY*X forward	Sigma Aldrich	5′-AGCACTGTCCTCTTCATGCTTT-3′
FY*B/FY*X reverse	Sigma Aldrich	5′-GCAGAGCTGCGAGTGCTAC-3′
LDR probes		
PRO ntT MTAG	Sigma Aldrich	5′-ACACTTATCTTTCAATTCAATTACcattagt ccttggctcttat-3′
PRO ntC MTAG	Sigma Aldrich	5′-CTTTCTCATACTTTCAACTAATTTtcattagt ccttggctcttac-3′
PRO common	Sigma Aldrich	5′-cttggaagcacaggcgctg-biotin-3′
FY*A ntG MTAG	Sigma Aldrich	5′-CAAACAAACATTCAAATATCAATCttccca gatggagactatgg-3′
FY*B ntA MTAG	Sigma Aldrich	5′-TACATTCAACACTCTTAAATCAAActtccca gatggagactatga-3′
Codon42 common	Sigma Aldrich	5′-tgccaacctggaagca-biotin-3′
FY*B ntC MTAG	Sigma Aldrich	5′-CACTTAATTCATTCTAAATCTATCtgcttttc agacctctctcc-3′
FY*X ntT MTAG	Sigma Aldrich	5′-ACTTATTTCTTCACTACTATATCAtgcttttc agacctctctct-3′
Codon89 common	Sigma Aldrich	5′-gctggcagctctgccctggct-biotin-3′
Surface Plasmon Resonance		
CM5 Sensor chip	Cytivia	29104988
Anti-DARC [2C3]	Absolute Antibody	https://absoluteantibody.com/product/anti-darc-2c3/Ab00893-10.0_human_igg1/standard/
ImageStream		
CellTrace CFSE Cell Proliferation Kit	Thermo Fisher	https://www.thermofisher.com/order/catalog/product/C34554
Höchst 33342	Life Technologies	H3570
Software		
FlowJo version 10.0	Becton Dickison & Company (BD)	https://www.bdbiosciences.com/en-us/products/software/flowjo-v10-software
BD FACSDiva™ Software version 8.0	Becton Dickison & Company (BD)	https://www.bdbiosciences.com/en-us/products/software/instrument-software/bd-facsdiva-software
WinList 9.0	Verity Software House	https://www.vsh.com/products/winlist/index.asp
STATA version 13.0	StataCorp LLC	https://www.stata.com/products/
Graphpad Prism version 10	GraphPad software, Inc.	https://www.graphpad.com/features
IDEAS Application Version 6.2.187	Amnis part of EMD Millipore	https://ideas.com/